Biomedical Materials Based on Electrospun Polymeric Fibers

by

Zhiwei Xie

A dissertation submitted to the Graduate Faculty of
Auburn University
in partial fulfillment of the
requirements for the Degree of
Doctor of Philosophy

Auburn, Alabama
December 13, 2010

Keywords: biomaterials, electrospinning, nanofibers, drug delivery, surface modification,

Approved by

Gisela Buschle-Diller, Chair, Professor of Polymer and Fiber Engineering
Peter Schwartz, Professor of Polymer and Fiber Engineering
Maria Lujan Auad, Assistant Professor of Polymer and Fiber Engineering
Xinyu Zhang, Assistant Professor of Polymer and Fiber Engineering

Abstract

As one of the most promising development of nanotechnology, electrospinning has gathered a great deal of interests in recent years. In this study, several novel nanomaterials were prepared by electrospinning and further modifications for future biomedical applications. Four projects were majorly covered in this dissertation with different focus on drug delivery or tissue engineering.

In the first project, poly(D,L-lactide) (PDLLA) was electrospun into ultrafine fibers and loaded with tetracycline (TC) or chlorotetracycline (CTC) as model drugs. The influence of a co-solvent (methanol) at various concentrations was studied regarding physical properties, morphology and in vitro release profiles of the drugs from the PDLLA nano-fibers. The results showed that, for both drugs, electrospun fiber diameters decreased with increasing amounts of co-solvent, while water contact angles and drug loading efficiency increased. However, the two drugs exhibited considerably different release mechanisms. The results indicated that the concentration of methanol changed the release profiles mainly based on the morphology of the resultant nano-fibers and the polymer/drug/solvent interaction during the electrospinning and drug release process.

In the second project, crystalline poly(L-lactide) (PLLA) nanoparticles were prepared by aminolysis of electrospun PLLA nanofibers and subsequently labeled by a fluorescent colorant. The size of the nanoparticles could be controlled by either the conditions of the aminolysis reaction or the diameter of the original electrospun fiber.

The latter method resulted in higher yield. Although the as-spun nanofibers were generally amorphous, the nanoparticles showed high crystallinity in the typical α-form of PLLA crystals. After aminolysis, PLLA nanoparticles spontaneously generated amine groups on the surface, which are available for further modifications. In this study the amine groups were reacted with isothiocyanate groups, and fluorescein-5'-isothiocyanate was successfully attached to the PLLA nanoparticles. Smaller particles showed significantly higher fluorescein binding density. Through this simple "top-down" routine, it was possible to create nanoparticles with tailorable size and specific surface functions. Such materials could potentially serve in bioimaging or nanomedicine applications.

In the third project, efforts were made to prepare nanofibrous poly(D,L)-lactide mats by electrospinning. However, it was observed that these mats tend to shrink under physiological conditions. Thus, a physical entrapment method to modify the polymer surface with poly(ethylene glycol) was developed to ensure dimensional stability and to increase the hydrophilicity of the surface of the mats. Nanofiber morphology was characterized by scanning electron microscopy. Surface element analysis was performed by high resolution X-ray photoelectron spectroscopy. Water contact angles were determined to identify surface properties before and after surface entrapment. Canine fibroblasts were prepared and seeded onto the poly(D,L)-lactide mats, followed by cell viability tests by MTT assay, which confirmed the improvement of biocompatibility by surface modification. Taking the results into account, hydrophilic and area-stable nanofibrous nonwoven mats were successfully produced, with potential applications as tissue engineering scaffolds.

In the last project, electrospun polymeric nanofibers were surface modified or surface coated chemically. As the first approach, electrospun poly(ε-caprolactone) was surface etched and further attached with biomolecules, e.g. chitosan and collagen. X-ray photoelectron spectrum confirmed the success of surface modification. For the second approach, polypyrrole (Ppy), which is a conducting polymer, was coated on electrospun PDLLA nanofibers via aqueous in-situ polymerization. The coating was characterized by electron microscopes and infrared spectroscopy. The resulted core-shell fibers had a wall thickness of 40-45 nm. By further removal of PDLLA, Ppy nanotubes were successfully fabricated. In summary, chemically modified electrospun nanofiber can provide unique surface properties, which is critique for tissue growth and regeneration.

Acknowledgments

The author would like to express his thanks to his advisor and mentor, Dr. Gisela Buschle-Diller, for her guidance, encouragement, support and valuable advice. The author is also grateful to his committee members, Dr. Peter Schwartz, Dr. Maria L. Auad and Dr. Xinyu Zhang for their suggestions and help.

The author is owed a tremendous appreciation to Dr. Xuehong Ren for his teachings, discussion and brilliant advices. Thanks also go to group members: M.A. Karasalan and Bo Yuan. Thanks to Dr. Tung S. Huang, Dr. Michael Bozack, and Dr. Curtis Bird for their help of testing. Thanks to the Department of Polymer and Fiber Engineering for providing support and exciting research environment.

He would like to express his most sincere thanks to his parents, Changzhong Xie and Lizhen Wen; his wife, Yawei Han, for the love and encouragement throughout the years.

Table of Contents

List of Tables

List of Figures

CHAPTER 1 INTRODUCTION

Introduction

Health has been a critical part of the quality of life since the start of human-being. Since half of a century ago, biomedical engineering, which is the combination of medical science and engineering principles, has contributed tremendously to improving the health care. One key issue of biomedical engineering is the materials being used, which are called biomaterials. Numerous materials, especially polymers, have been utilized as biomaterials to replace or enhance an organ or tissue of the human body. As the development of biomaterials proceeds, the third generation biomaterials require to be not only biocompatible and bioactive, but also bioresorbable.

Nanomaterials have been an exciting development in materials science in the past two decades. Nanomaterials exhibit new properties, while the dimensions of materials decrease. Polymeric nanomaterials can provide unique properties and large surface contact area essential for biomedical applications, especially in the area of controlled drug delivery and tissue engineering. For example, polymer nanoparticles can penetrate same biological membranes to some specific location that need treatment due to their small size. Moreover, polymer scaffold with nanopores can have extremely large surface area, which is suit for cell growth and further for tissue engineering.

One significant technique of nanotechnology that has been studied extensively in recent years is electrospinning. A high-voltage electrical field is used to format fibers

from polymer solutions with extremely high elongation ratio in a relative short spinning distance. It is an easy and versatile method to fabricate ultrafine fibers with diameter as low as a few nanometer. Due to the large surface area of polymeric nanofibers, they can be applied as filters, membranes, catalysts, sensors, and biomedical materials, which are emphasized in this research. In addition, electrospun nanofibers are structurally similar to the extracellular matrix (ECM), which is the support of cell proliferation *in vivo*. Thus electrospinning could be a promising technique to prepare novel nanomaterials for biomedical applications.

Objective

The overall goal of this work is to fabricate and modify electrospun nanofibers into different formations intended for varied biomedical applications. Generally, the whole study consists of four projects. Two of them emphasize drug delivery, while other two at for tissue engineering applications. For drug delivery, a monolithic system of nanofibers was prepared and the drug release profiles were controlled by varying solvent systems used for electrospinning. The second project of drug delivery was to create some nanoparticles from electrospun nanofiber via a “top-down” routine. Furthermore, the possibility to attach small molecules to the product nanofibers was proved. On the other hand, although electrospun nanofibers have large surface area to support cell growth, the surface chemistry and properties need to be tailored for real tissue engineering applications. Thus the last two projects were conducted by physical and chemical surface

modifications after electrospinning. The idea was to generate better surface properties or novel nanostructures.

Chapter arrangement

The dissertation is divided into six chapters. Chapter 1 is the introduction of the topic and objective. Chapter 2 reviews the existing literature in the related area of biomaterials and electrospinning. Chapters 3 to 6 are the major body of each project in the sequence of monolithic drug delivery, nanoparticles, physical surface modification and chemical surface modification. Each chapter consists of an introduction, experimental section, results and discussion, and a conclusion.

CHAPTER 2 LITERATURE REVIEW

2.1 Biomaterials and biomedical engineering

The development of biomedical engineering started roughly 50 years ago. The application of engineering principles and techniques to the medical field has ever since played an important role in healthcare. With the combination of the design and problem solving skills of engineering in medical and biological sciences, biomedical engineering improved the quality of life in many aspects of healthcare diagnosis and treatment [1]. Generally, biomedical engineering comprises several disciplines, including biotechnology (a board and even ambiguous concept), tissue engineering, genetic engineering, pharmaceutical engineering, medical device development, medical imaging, and development and application of biomaterials.

In a broad sense, the materials used in the biomedical field are called biomaterials. People have been using biomaterials since thousand years ago; however, the modern development of biomaterials is strictly speaking not a new area of science, having existed for around half a century [2]. There are two major definitions for biomaterials. Traditionally, biomaterial is defined as “A biomaterial is any material, natural or man-made, that comprises whole or part of a living structure or biomedical device which performs, augments, or replaces a natural function” [2]. However, Williams’ definition,

which is “a biomaterial is a nonviable material used in a medical device, intended to interact with biological systems”, is more commonly accepted by modern biomaterial research society [3]. Moreover, biomaterials science encompasses elements of medicine, biology, chemistry, tissue engineering and materials science.

During the 1960s and 1970s, biomaterials were mostly “ad hoc” inert materials being used as implants. Then, researchers shifted their focus from inert components to bioactive or bioresorbable materials that could elicit a controlled action and reaction in the physiological environment. The materials developed during this period were known as the second generation of biomaterials. Right now, we are on the era of third generation biomaterials, which require both bioactivity and bioresorbability, with the aim that once implanted, will help the body heal itself [4].

Until now, most kind of natural and synthetic materials have been used as biomaterials, including metals, ceramics, polymers and composites [5]. Especially synthetic polymeric materials have been extensively utilized in medical disposable supplies, prosthetics, dental materials, implants, drug delivery and tissue engineering [6]. Not all polymers can be applied as biomaterials; polyethylene (PE), polyethylenterephthalate (PET), polytetrafluorethylene (PTFE) and polyurethane (PU) are most commonly seen. In order to meet the requirements of the third generation biomaterials, biodegradable polymers have been intensively studied in recent years. Polylactide (PLA), polyglycolide (PGA), polycaprolactone (PCL), polyhydroxyalkanoates (PHAs), and their copolymers are some significant examples [6].

With the development of materials science, biomaterials have been contributing a lot to help improving the quality of healthcare and the quality of life. One of the major breakthroughs is the application of nanotechnology, which will be discussed in the next section.

2.2 Nanomaterials and nanotechnology

In past two decades, “nano” has become a buzz word in both science and engineering. The federal government of the United States spent billions of dollars in recent years in research for nanomaterials and nanotechnology. A similar trend was true for Europe, Japan, China and many other countries. “Nano” is a big growing business also. The National Foundation of Science predicted that by the year of 2015, the nano-market will be reach around $1 trillion [7].

A restrictive definition of nanomaterials is that nanomaterials have properties which change tremendously upon becoming smaller. However, the most accepted definition of nanomaterials in scientific fields is that materials that have sizes below 100nm, at least in one dimension are considered “nanomaterial”. The technology applied to synthesis, process, analysis and use of nanomaterials is called nanotechnology. It is an intersection of several disciplines, including chemistry, physics, biology, materials science [8].

Actually, for materials, size is a decisive factor; materials with reduced size can show different properties compared to the bulk with potential unique applications. For example, opaque substances become transparent (copper); stable materials turn

combustible (aluminum); insoluble materials become soluble (gold) [9]. On the other hand, nanomaterials also provide a very large surface area at the same mass.

To produce nanomaterials, two major routines were commonly utilized. The first one is "bottom-up", while most macroscale materials were made by "top-down" approach. Generally, "bottom-up" technology seeks to arrange smaller components into more complex assemblies in nanoscales. For instance, molecular self-assembly takes advantages in supramolecular chemistry, and molecular recognition, to guide some small molecular components to automatically arrange themselves into some regular nano-conformation [8]. On the other hand, "top-down" methods are also capable of fabricating nanomaterials. Nanolithography, which normally uses chemicals or light to pattern the surface of a material in less than 100 nm scale, is a great example of this approach.

The rapid development of nanomaterials was greatly benefited from modern characterization techniques. Not only the modification of traditional analysis techniques, like X-ray diffraction (XRD), small angle X-ray scattering (SAXS), scanning and transmission electron microscopy (SEM and TEM), has had significant impact, but also the development of the atomic force microscopy (AFM) and the scanning tunneling microscopy (STM) became novel tools of nanotechnology [10].

Until now, numerous kinds of nanomaterials have been created, including nanoparticles (both inorganic and polymeric), nanorods, nanowires, nanotubes (especially carbon nanotubes), nanofibers, nanofilms, nano-electromechnical systems (NEMS), and much more. They have been widely used in electronics, optical devices, energy, composites, consumer goods, medicines and health treatments [11]. Besides the effort of

creating new nanomaterials and reducing the cost of manufacture, safety and environmental concerns are some other major issues in this area [12].

2.3 Nanotechnology in drug delivery and tissue engineering

The applications of nanotechnology in the biomedical area have gained tremendous interests in recent years. In most cases, nanostructures were applied in controlled drug delivery system or tissue engineering scaffolds [13].

Modern therapeutics is taking great advantages from controlled drug delivery system, in which polymers are important components. Normally, “control” means two different aspects. The first aspect is the capability to deliver a specific drug to a desired location, while could be a tissue, an organ, or an illness site. Another meaning of controlled drug delivery is managing the drug concentration with the system of circulation to avoid toxic side effects while maintain drug effectiveness [2]. Polymeric nanoparticles are outstanding candidates for controlled drug delivery. Their small size enables them to penetrate certain biological membranes and due to their large surface area they can be attached to proteins, antibodies, and other recognition units [14]. Moreover, polymers can be easily fabricated into core-shell particles and dentrimers, which are potentially available for future drug or gene delivery [15]. Biodegradable polymers and copolymers also play a significant role to administer the drug release rate [16]. Nanofibers are another promising carrier for controlled delivery of therapeutic molecules [17], which will be discussed later in more details.

Tissue engineering is another notable application of nanotechnology in biomaterials area. It is defined as “a set of tools at the interface of the biomedical and engineering sciences that use living cells or attract endogenous cells to aid tissue formation or regeneration, and thereby produce therapeutic or diagnostic benefit” [2]. A tissue or organ can be repaired or reconstructed by growing living cells on a polymeric scaffold *in vivo*, or *in vitro*. Thus, the polymeric scaffold needs not only to be biocompatible and bioactive, but also to have a porous structure with large surface area. Therefore, nanofibers and injectable nanoparticles as cell carriers are two vivid candidates in this area [18, 19]. Also, surface modification of existing biomaterials in nanoscale could improve the performance significantly [20].

2.4 Basics of electrospinning

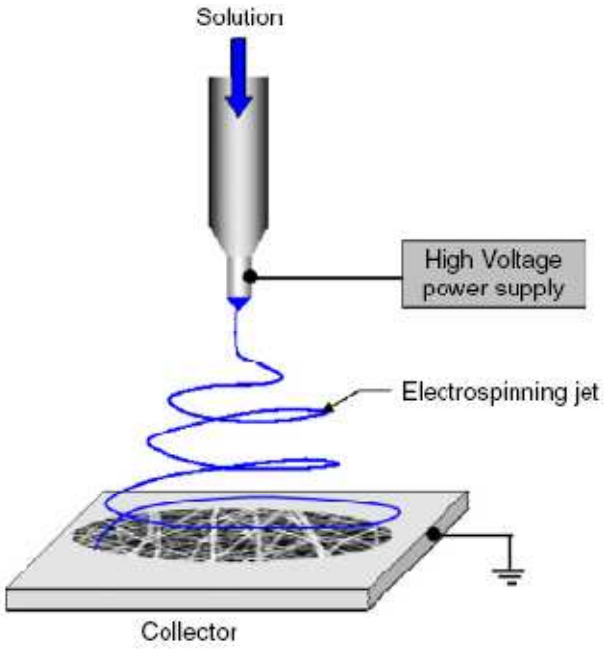

Figure 2.1 A typical setup of electrospinning [29]

With the combination of nanotechnology and macromolecular science, polymer nanomaterials have gained a great deal of research interests and real-life applications in the past several decades [21-22]. Among all techniques to create polymer nanofibers, electrospinning is one of the most promising approaches, since it is easy, versatile and cheap [23]. Normally, polymer solutions [24] and melts [25] can be produced into fibrous structures like non-wovens with fiber diameter from several nanometers to a few microns. Currently, it is the only technique to generate continuous fibers with diameter of a few nanometers [26]. Since be discovered by Cooley [27] and Morton [28], especially in the recent 15 years, electrospun nanofibers have been applied in several different fields, for example, for filtration, sensors, protective clothes, membranes, drug delivery, wound healing and tissue engineering [23, 26, 29].

The basic setup of electrospinning is relatively simple. Both polymer solution, which is easier and more common, and polymer melt can be used for electrospinning. For a single jet electrospinning process, a horizontal or vertical (as shown in Figure 2.1 [29]) experimental setup can be applied, consisting of a syringe, a needle, a grounded collecting board, and a high voltage supply. A syringe pump connected to the syringe controlls the flow rate. When high voltage (normally 5kV-50kV) is applied between the tip of the needle and the collector, polymer jet will be driven by an electrical field to form ultrafine fibers on the collecting board.

Since 1990's, electrospinning has gained a significant amount of interests from academic researchers. As shown in Figure 2.2, publications and patents related to electrospinning increased tremendously in recent years. For 2009 alone, 1646 papers

were published in this area. From this aspect, it can be demonstrated how fascinating this technique is. Thus, the opportunities are unlimited in this area.

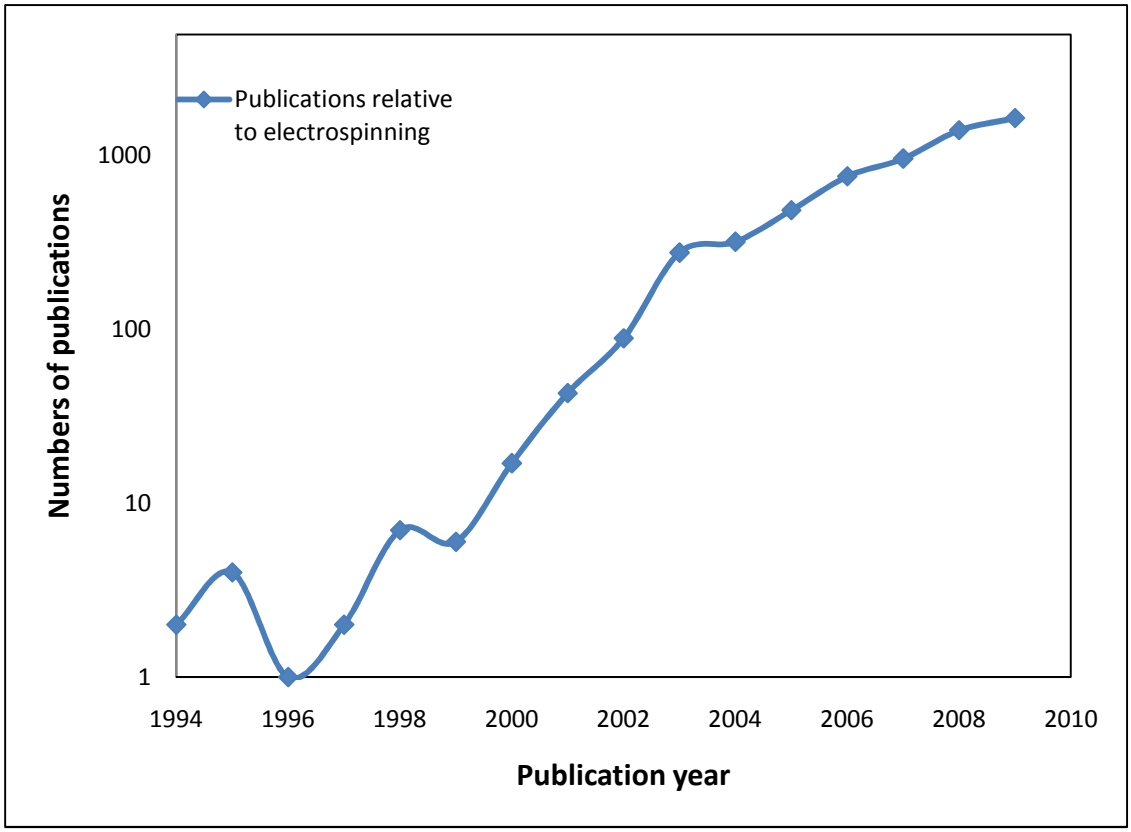

Figure 2.2 Numbers of publications and patents with keyword of "electrospinning". Data acquired from Scifinder Scholar 2007 ®.

Although the setup seams to be simple, the mechanism of electrospinning is rather complicated. In general, the process can be described as the interaction of several instability processes caused by surface tension, electrical force and other parameters [30]. The major driving force for the fiber formation from solution jet is called Rayleigh instability. A periodic pearl-necklace formation composed of drops is the final state of the Rayleigh instability. Another two important instabilities, which are known as axisymmetrical instability and the bending (or whipping) instabilities, are induced by the

coupling of the solution jet with the electric field [30]. Axisymmetrical instability is the cause of beads structure formation, which can be prevented by variation of electrospinning conditions. Bending instability causes the solution jets to loop towards the collector, instead of straightly spraying on. So the stretching ratios are about 10^5, which is the reason small fiber diameters can be generated by electrospinning.

Table 2.1 Effects of electrospinning parameters on fiber formation [31-35]

Parameter		Effects
Process parameters	Applied voltage	Must be high enough to form Taylor cone. Too weak or too strong will lead to beads.
	Flow rate	Pore size, beads formation.
	Spinning distance	Fiber diameter, beads formation
Solution parameters	Solution concentration	Dominating factor of spinnability, fiber diameter
	Solvent volatility	Surface morphology, beads formation
	Solution conductivity	Spinnability, fiber diameter
	Molecular weight	Lowest concentration can form fibers
Environmental parameters	Humidity	Surface morphology

Although electrospinning is a dynamic procedure, researchers have found some effective methods to control the process by changing several parameters. Firstly, the properties of the polymer solution are most important. Secondly, processing parameters

are another significant aspect that determines the final products' properties. Thirdly, environmental conditions are non-negligible. The influence of each parameter is summarized in Table 2.1 [31-35].

With the development of the electrospinning technique, it is not only a method to fabricate nanofibrous non-woven mats, but also to form more complicated and designed nanostructures, for example, core-sheath nanofibers by co-axial electrospinning [36], well-aligned nanofibers by designed formation of the collector board [37], 3-dimensional nanofiber/microfiber composites [38]. Also other organic, inorganic or even biological nanorods, nanotubes can be aligned by encapsulating into electrospun fibers [39]. Until now, most researchers reported the diameters of electrospun fibers to be in the range of a few hundred nanometers to one or two microns. Huang et al, [40] successfully prepared nanofibers with a diameter of 1.6 nm; however, it is still challenging to electrospin such thin and uniform fibers in a larger amount. The versatility of this method gives us an opportunity to produce intricate nanomaterials in a cheap, easy and continuous manner. Essentially, use modified electrospinning technique and the use of electrospun fibers as templates for further treatment are still attractive topics in this area.

However, for real industrial production, the mass productivity is the key issue. Some pioneers tried to fabricate electrospun fibers in large amounts and increased the spinning speed by multi-jet electrospinning [41], needle-less electrospinning [42] or bubble-assist electrospinning [43]. There are some commercialized electrospinning machines on the market [44, 45]; however some continuous manufacture and quality control problems are still remaining.

2.5 Applications of electrospinning

Due to the ease of manufacturing, versatility, the high surface area, and high porosity of the products and many other benefits, electrospinning has been applied to many areas as above-mentioned. In this section, these methods will be discussed in more detail.

Electrospun non-woven mats have gained widespread interests since last 5-10 years, because the porous structure could be a scaffold for cell growth and the fibrous formation could be a mimic of the extracellular matrix (ECM) [31]. On the other hand, since the electrospinning process is relatively slow and low in producing, it makes sense to first apply electrospun fibers in the biomedical field, especially in drug delivery and tissue engineering.

2.5.1 Drug delivery

Electrospinning provides great flexibility in selecting matrix materials for drug delivery. Both degradable and non-degradable polymers can be electrospun into nanofibers and loaded with drugs. Accordingly, due to the varied material selection variety of drugs can be encapsulated including: antibiotics, anticancer drugs, proteins, and DNA. The formation of drug delivery system can be changed also, for example, into a monolithic system by electrospinning of a mixture of drug and polymer solution and reservoir system by co-axial electrospinning. These techniques can be used to control the drug release kinetics [31].

Since Kenawy et al,. [46] first successfully electrospun poly(ethylene-co-vinylacetate), poly (lactic acid) and blends thereof with tetracycline hydrochloride, more than 50 different electrospun drug delivery systems have been studied, most of them were just performed *in vitro*. Currently, the major opportunity for this area will be in real *in vivo* applications. The drug loaded fibrous mats can be used as transdermal drug delivery, wound dressing, and direct local attachments. So for the next step, the better understanding of drug/polymer/tissue interaction is critical, since both drug encapsulation and fiber formation controllability have already been proven [47]. Further, drug diffusion into body circulation is another significant issue. With more *in vivo* tests, the electrospinning process can be designed to obtain the desired drug release profiles.

2.5.2 Tissue engineering

As a structural mimic of extracellular matrix, electrospun nanofibers have been studied as scaffold for cell growth in the area of tissue engineering and tissue regeneration [48-51]. A great number of polymers, including biodegradable polymers (e.g., polylactide), non-degradable polymers (e.g., polyurethane) and natural polymers (e.g., collagen), have been electrospun into porous non-woven mats to support cell proliferation. Most of the research was focused on skin, blood vessel, bone, nerve and cartilage tissue engineering,

Attempts to replicate complicated nature of native ECM have led to electrospinning of a wide range of fiber formations and compositions, as well as tailored biological, chemical and mechanical properties of the nanofibers. Qiu and coworkers [52] synthesized and electrospun copolymers of caprolactone and lactide nanofibers as scaffolds for vascular tissue engineering. Ma et al, [53] also surface modified electrospun

PET fibers intended for blood vessel engineering. A rotating frame cylindrical collector was used by Zhu et al, [54] to produce highly porous nanofiber mats for skin tissue engineering. Chen et al, [55] proved that electrospun collagen/chitosan nanofibers had both biocompatibility and activity for wound healing. Prabhakaran and coworkers [56] prepared PCL/collagen nanofibers by electrospinning in aim of nerve tissue engineering. Pure hydroxyapatite (HA) nanofibers were made by electrospinning and further removal of polymers. The resulting HA fibers are highly crystallized and capable to guide bone regeneration [57]. Researchers also immobilized growth factors on electrospun poly(lactic-co-glycolic acid) (PLGA) as tendon and cartilage tissue scaffolds [58].

Thus, the capability to generate porous structures with large surface area and versatility to modify bulk and surface properties makes electrospun nanofibers great candidates for tissue engineering applications.

2.5.3 Antibacterial materials

Electrospun nanofibers containing antibacterial agents also can be prepared in an easy and feasible way. Jin et al, [59] directly incorporated silver nanoparticles in polymer solution, and then conducted electrospinning to make nanofibrous mats with excellent biocidal activity. Silver nitrate were also incorporated in polymer nanofibers by electrospinning, and further reduced into Ag nanoparticles [60]. Silver-imidazole complexes also enhanced their antibacterial performance by being loaded in electrospun fibers [61]. The fiber mats slowly released nanosilver, and as a result, showed sustained bacteria killing behavior. Ren and coworkers [62] loaded N-halamine onto

polyacrylonitrile nanofibers with “rechargeable” antibacterial activity. This research showed that electrospun fiber mats could be fascinating carriers for biocidal materials.

2.5.4 Filters and membranes

With controllable porous structure and fiber surface morphology, electrospun non-woven mats are a promising material for filtration applications, even ultrafiltration. Polysulfone [63], poly(vinyl alcohol) [64], poly(acrylonitile) [65], and other polymers have been applied in order to separate particles or solvent from bulk. Among them, the most efficient and realizable technique is the multi-layers setup [64-65]. The support layer provides mechanical strength, and the electrospun layer with controllable pore size (with changing of fiber diameters) exhibits the ability of separating water and oil, while a water-resistant but water-permeable chitosan coating protects the whole membrane. The oil rejection efficiency was higher than 99.9% even after 24 h usage.

With the help of particle decoration [66] and co-axial electrospinning [67], superhydrophobic membranes can be fabricated. These electrospun membranes could be potentially useful not only in ultrafiltration, but also as self-cleaning textiles and construction materials. Electrospun proton exchange polymers are also good candidates for fuel cells membranes [68]. Furthermore, TiO_2 nanofibrous membranes were prepared via electrospinning with removable polymer template, intended for photovoltaic applications [69] and solar cells [70].

2.5.5 Sensors

Taking advantage of their high surface area and good transport properties, the electrospun nanofibers have been investigated as a variety of sensors, including chemical sensors [71], optical sensors [41], and biological sensors [72, 73]. There are two major approaches, direct electrospinning of active polymers, or loading/conjugating active compounds, including reactive small molecules, fluorescent dyes or dots, and enzymes, on electrospun fibers. Aligned electrospun fibers showed even higher sensitivity and selectivity [74]. Yoon et al, [75] successfully electrospun polydiacetylene-embedded nanofibers and used them as a colorimetric assay for organic solvents.

2.5.6 Catalysts

Similar to sensor applications, with reactive compounds, electrospun nanofibers can be used as catalysts or catalyst support [76-78]. It is well known that the catalyst is more active with increasing the surface area of the catalyst per unit volume. As mentioned above, one of the important advantages of nanofibers is their high surface areas, which make them tremendously applicable in modern catalysis. Zhang et al, [79] prepared Fe-TiO_2/SnO_2 hybrid nanofibers by electrospinning as a photocatalyst for environmental remediation. Electrospun nanofiber can also play a protective role in maintaining the activity of the nano-catalyst [80]. Not only organic and inorganic catalysts can be loaded on electrospun fibrous mats, but also enzymes and other bio-catalysts. For example, lipase was successfully immobilized on polystyrene nanofibrous mats by Sakai and coworkers [81] with enhanced performance.

In summary, as an old technique with significant modern developments, electrospinning is a significant tool for varied nanomaterials in the future, not only owing

to it being a simple, versatile, and straightforward procedure, but also due to the potential applications in a wide range of areas. With the great opportunities and challenges, only the sky will be the limit for the creativity of electrospinning.

2.6 References

1. Bronzino J.D. Biomedical Engineering fundamentals; Taylor & Francis Group: Boca Raton, FL, 2006.
2. Ratner B.D.; Hoffman A.S.; Schoen F.J.; Lemons J.E. Biomaterials science: An introduction to materials in medicine; Elsevier: London, 2004.
3. Williams D.F. Definitions in Biomaterials. Proceedings of a consensus conference of the European society for biomaterials; Elsevier: New York, 1987, Vol.4.
4. Hench L.L.; Polak J.M. Science 2002, 295, 1014.
5. Dee K.C.; Puleo D.A.; Bizios R.; An introduction to Tissue-Biomaterial interactions; John Wiley & Sons: Hoboken, NJ, 2002.
6. Park J.B.; Bronzino J.D. Biomaterials: Principles and applications; CRC Press: Boca Raton, FL, 2003.
7. Ratner M.A.; Ratner D. Nanotechnology: a gentle introduction to next big idea; Pearson Education: Upper Saddle River, NJ, 2003.
8. Vollath D. Nanomaterials: an introduction to synthesis, properties and applications; Wiley-VCH: Weinheim, Germany, 2008.
9. Lubick N. Environ. Sci. Technol. 2008, 42, 3910.
10. Gao G. Nanostructures and nanomaterials; Imperial College Press: London, UK,

2004.

11. Gogotsi Y. Nanomaterials Handbook; CRC Press: Boca Raton, FL, 2006
12. Oberdörster G.; Oberdörster E.; Oberdörster J. Environ. Health Perspec. 2005, 113, 823.
13. Goldberg M.; Larger R.; Jia X. J. of Biomater. Sci., Polym. Edn. 2007, 18, 241.
14. Kaparissides C; Alexandridou S.; Kotti K.; Chaitidou S. J. of Nanotechnol. 2006, 2, 1.
15. Nishiyama N.; Kataoka K. Pharma. & Therap. 2006, 112, 630.
16. Panyam J.; Labhasetwar V. Adv. Drug Delivery Rev. 2003, 55, 329.
17. Kumbar S.G.; Nair L.S.; Bhattacharyya S.; Laurencin C.T. J. of Nanosci. And Nanotechnol. 2006, 6, 2591.
18. Sill T.J.; von Recum H.A. Biomaterials 2008, 29, 1989.
19. Kretlow J.D.; Young S.; Klouda L.; Wong M.; Mikos A.G. Adv. Mater. 2009, 21, 3368.
20. Kasemo B. Surface Sci. 2002, 500, 656.
21. Ober C.K.; Cheng S.Z.D.; Hammond P.T.; Muthukumar M.; Reichmanis E.; Wooley K.L.; Lodge T.P. Macromolecules 2009, 42, 465.
22. Hammond P. T. Adv. Mater. 2004, 2, 1271.
23. Schiffman J.D.; Schauer C.L. Polym. Rev. 2008, 48, 317.
24. Reneker D.H.; Chun I. Nanotechnology 1996, 7, 216.
25. Dalton P.D.; Grafahrend D.; Klinkhammer K.; Klee D.; Möller M. Polymer 2007, 48, 6823.

26. Greiner A.; Wendorff J.H. Angew. Chem. Int. Edn. 2007, 46, 5670.

27. Cooley J.F. US Patent Specification 692631, 1902.

28. Morton W.J. US Patent Specification 705691, 1902.

29. Teo W.E.; Ramakrishna S. Nanotechnology 2006, 17, R89.

30. Yarin A.L.; Koombhongse S.; Reneker D.H. J. Appl. Phys. 2001, 89, 3018.

31. Sill T.J., von Recum H.A., Biomaterials, 2008, 29, 1989.

32. Deitzel J.M.; Kleinmeyer J.; Harris D.; Tan N.C.B. Polymer 2001, 42, 261.

33. Meechaisue C.; Dubin R.; Supaphol P.; Hoven V.P.; Kohn J. J. Biomater. Sci. Polym. Edn. 2006, 17, 1039.

34. Megelski S.; Stephens J.S.; Chase D.B.; Rabolt J.F. Macromolecules 2002, 35, 8456.

35. Zhang C.X.; Yuan X.Y.; Wu L.L.; Han Y.; Sheng J. Eur. Polym. J. 2005, 41, 423.

36. Sun Z.; Zussman E.; Yarin A.L.; Wendorff J.H.; Greiner A. Adv. Mater. 2003, 15, 1929.

37. Li D.; Wang Y.; Xia Y. Adv. Mater. 2004, 16, 361.

38. Kim S.J.; Jang D. H.; Park W.H.; Min B-M. Polymer 2010, 51, 1320.

39. Ko F.; Gogotsi Y.; Ali A.; Naguib N.; Ye H.; Yang G.L.; Li C.; Willis P. Adv. Mater. 2003, 15, 1161.

40. Huang C.; Chen S.; Lai C.; Reneker D.H.; Qiu H.; Ye Y.; Hou H. Nanotechnology 2006, 17, 1558.

41. Wang X.; Lee S-H.; Ku B-C.; Samuelson L.A.; Kumar J. J. of Macromol. Sci. pure & appl. Chem. 2002, A39, 1241.

42. Park J.C. U.S. Patent specification 20080241297, 2006

43. Yarin A.L.; Zussman E. Polymer 2004, 45, 2977.

44. http://www.nanostatics.com/

45. http://www.mecc.co.jp/en/html/products/nanon.html

46. Kenawy E-R.; Bowlin G.L.; Mansfield K.; Layman J.; Simpson D.G.; Sanders E.H.; Wnek G.E. J. of Controlled Release 2002, 81, 57.

47. Liang D.; Hsiao B.S.; Chu B. Adv. Drug Delivery Rev. 2007, 59, 1392.

48. Liao S.; Li B.; Ma Z.; Wei H.; Chan C.; Ramakrishna S. Biomed. Mater. 2006, 1, R45.

49. Sell S.; Barnes C.; Smith M.; McClure M.; Madurantakam P.; Grant J.; McManus M.; Bowlin G. Polym. Int. 2007, 56, 1349.

50. Yang F.; Murugan R.; Wang S.; Ramakrishna S. Biomaterials 2005, 26, 2603.

51. Li W-H.; Tuli R.; Okafor C.; Derfoul A.; Danielson K.G.; Hall D.J.; Tuan R.S. Biomaterials 2005, 26, 599.

52. Qiu R-X.; Li C-M.; Ye L.; Dong J-D.; Zhang A-Y.; Gu Y-Q.; Feng Z-G. Biomed. Mater. 2009, 4, 004105.

53. Ma Z.; Kotaki M.; Yong T.; He W.; Ramakrishna S. Biomaterials 2005, 26, 2527.

54. Zhu X.; Cui W.; Li X.; Jin Y. Biomacromolecules 2008, 9, 1795.

55. Chen J-P.; Chang G-Y.; Chen J-K. Coll. & Surf. A: Physicochem. Eng. Aspects 2008, 313-314, 183.

56. Prabhakaran M.P.; Venugopal J.; Chan C.K.; Ramakrishana S. Nanotechnology 2008, 19, 455102.

57. Kim H.W.; Kim H.E. J. Biomed. Mater. Res, B: Appl. Biomater. 2005, 77, 323.

58. Sahoo S.; Ouyang H.; Goh J.C.H.; Tay T.E.; Toh S.L. Tissue Eng. 2006, 12, 91.

59. Jin W-J.; Lee H.K.; Jeong E.H.; Park W.H.; Youk J.H. Macromol. Rap. Commun. 2005, 26, 1903.

60. Son W.K.; Youk J.H.; Lee T.S.; Park W.H. Macromol. Rap. Commun. 2004, 25, 1632.

61. Melaiye A.; Sun Z.; Hindi K.; Milsted A.; Ely D.; Reneker D.H.; Tessier C.A.; Youngs W.J. J. Am. Chem. Soc. 2005, 127, 2285.

62. Ren X.; Akdag A.; Zhu C.; Kou L.; Worley S.D.; Huang T.S. J. of Biomed. Mater. Res. A 2008, 91A, 385.

63. Gopal R.; Kaur S.; Feng C.Y.; Chan C.; Ramakrishna S.; Tabe S.; Matsuura T. J. of Membr. Sci. 2007, 289, 210.

64. Wang X.; Chen X.; Yoon K.; Fang D.; Hsiao B.S.; Chu B.; Environ. Sci. & Tech. 2005, 39, 7684.

65. Yoon K.; Kim K.; Wang X.; Fang D.; Hsiao B.S.; Chu B. Polymer 2006, 47, 2434.

66. Ma M.; Gupta M.; Li Z.; Zhai L.; Gleason K.K.; Cohen R.E.; Rubner M.F.; Rutledge G.C. Adv. Mater. 2007, 19, 255.

67. Han D.; Steckl A.J. Langmuir 2009, 25, 9454.

68. Bajon R. J. of Fuel Cell Sci. & Tech. 2009, 6, 5.

69. Onozuka K.; Ding B.; Tsuge Y.; Naka T.; Yamazaki M.; Sugi S.; Ohno S.; Yoshikawa M.; Shiratori S. Nanotechnology 2006, 17, 1026.

70. Jo S.M.; Song M.Y.; Ahn Y.R.; Park C.R.; Kim D.Y. J. of Macromol. Sci A: Pure & Appl. Chem. 2005, 42, 1529.

71. Kessick R.; Tepper G. Sensor & Actuator B: Chemical 2006, 117, 205.

72. Wang X.; Kim Y-G.; Drew C.; Ku B-C.; Kumar J.; Samuelson L.A. Nano Let.

2004, 4, 331.

73. Kowalczyk T.; Nowicka A.; Elbaum D.; Kowalewski T.A. Biomacromolecules 2008, 9, 2087.

74. Wang W.; Huang H.; Li Z.; Zhang H.; Wang Y.; Zheng W.; Wang C. J. of Am. Ceram. Soc. 2008, 91, 3817.

75. Yoon J.; Jung Y-S.; Kim J-M. Adv. Funct. Mater. 2009, 19, 209.

76. Kim H.; Choi Y.; Kanuka N.; Kinoshita H.; Nishiyama T.; Usami T. Appl. Catalyts A 2009, 352, 265.

77. Park S.H.; Jo S.M.; Kim D.Y.; Lee W.S.; Kim B.C. Syn. Metals 2005, 150, 265.

78. Demir M.M.; Gulgun M.A.; MencelogluBurak Y.Z.; Abramchuk E.S.; Makhaeva E.E.; KhokhlovValentina A.R.; Matveeva G.; Sulman M.G. Macromolecules 2004, 37, 1787.

79. Zhang R.; Wu H.; Lin D.; Pan W. J. Am. Ceram. Soc. 2010, 93, 605.

80. Xu X.; Wang Q.; Choi H.C.; Kim Y.H. J. of Membr. Sci. 2010, 348, 231.

81. Sakai S.; Yamaguchi T.; Watanabe R.; Kawabe M.; Kawakami K. Cataly. Commun. 2010, 11, 576

CHAPTER 3 ELECTROSPUN POLY(D, L-LACTIDE) FIBERS FOR MONOLITHIC DRUG DELIVERY SYSTEM

3.1 Introduction

In the past several years, polymer based controlled drug delivery systems have gained great attention due to the improvement of therapeutic efficacy and reduction of toxic side effects [1, 2]. Different types of drugs have been encapsulated into polymer micro-/nano-particles, hydrogels, films and other specific devices to deliver a particular medicine to a designated part of the body with a designed release pattern [2-5].

The formation of ultra-fine fibers with diameters in submicron to nanometer range by electrospinning has increasingly become important in recent years. Ultra-fine polymer fibers can be produced by using the electrostatic force between a spinneret and a grounded collector. It has been acknowledged that the jet instability is the main driving force for their formation [6, 7]. Electrospun non-woven fiber mats with a very large surface area to volume ratio find a wide range of biomedical applications in different areas, including tissue engineering, wound healing and drug release [8-10].

A variety of research has been reported in literature in regard to delivery systems, using model pharmaceutical compounds. For example, in an early study Kenawy et al,. [11] first successfully electrospun poly(ethylene-co-vinylacetate) (PEVA), poly (lactic

acid) (PLA) and blends thereof with tetracycline hydrochloride (TC). In other studies, the hydrophilic antibiotic drug Mefoxin was included in electrospun PLA (Zong et al,. [12]) and in poly(lactide-co-glycolide) (PLGA) matrices (Kim et al,. [13]). However, a reoccurring problem seemed to have been the relatively fast initial release of the pharmaceuticals. Later, model drugs have been encapsulated in core-shell nanofibers by Huang et al,. [14] and Liao et al,. [15] with a more sustained release profile. Chunder et al,. [16] successfully electrospun two weakly electrolytic polymers, poly(acrylic acid) (PAA) and poly(allylamine hydrochloride) (PAH), containing methylene blue. Temperature sensitive PAA/poly(N-isopropylacrylamide) (PNIPAAM) multi-layers were deposited onto the drug-loaded nano-fibers to control the release of drugs [16]. Moreover, electrospun fibers were fabricated as a delivery medium for proteins by Chew et al,. [17] as well as Zeng et al,. [18]. Recently, electrospun blend polymer fibers were also fabricated as carriers for paracetanol and ketoprofen, respectively, by Pend et al,. [19] and Kenawy [20]. Xie et al,. [21] used electrospun PGLA fibers with different diameters for the delivery of Paclitaxel which is used to treat C6 Glioma. In their study, a cytotoxicity test was performed to confirm the safe use of drug-loaded nano-fibers.

Although numerous reports are published concerning the incorporation of pharmaceutical compounds in nano-fibers, only few studies focus on the mechanism of controlled drug release and the corresponding release profile. Zeng et al,. [22] primarily investigated the solubility and compatibility of drugs in poly(L-lactide) (PLLA) ultrafine fibers. It was found that by choosing compatible drugs with PLLA, burst release could be avoided. Various drugs were also incorporated into nano-fibers by Taepaiboon et al,. [23]. Their research indicated that with increasing molecular weight of the drug, the overall

rate and the total amount of liberated drug decreased. Most recently, Srikar et al,. [24] performed a study to describe the release mechanism of a water-soluble compound from electrospun polymer fibers. The authors suggested that only the small molecules attached to the fiber surface could be released. The mechanism could then be described as a desorption-limited rather than a simple diffusion controlled process. However, there has been no report on the influence of drug solubility, the choice of the solvent for the electrospinning system, or the polymer/drug interaction in relation to the drug release profile from nanofibers.

In this study, the controlled delivery of two structurally similar model drugs, tetracycline hydrochloride (TC) and chlorotetracycline hydrochloride (CTC), from electrospun poly(D,L-lactide) (PDLLA) nanofibers was investigated. An effort was made to control the availability of the embedded drugs, and thus the fiber properties, by the solvent system used for electrospinning. The impact of the solvent system on changes in morphology and physical properties of the nano-fibers was studied to get a better understanding of the release mechanism. Finally, a possible mechanism of the drug release from electrospun fibers is suggested, considering drug/polymer/solvent interactions.

3.2 Experimental Section

3.2.1 Materials

Poly(D,L-lactide) (PDLLA, Mw = 75,000~120,000), chlorotetracycline hydrochloride (CTC), and tetracycline hydrochloride (TC) were obtained from Sigma-

Aldrich and used as received. The solubility of CTC and TC in methanol is 17.4 mg/mL and 50.0 mg/mL respectively. Chloroform (analytical grade) was obtained from Fisher Scientific and methanol (HPLC grade) from Sigma-Aldrich. 0.05 M Tris buffer solution was prepared from tris(hydroxymethyl)aminomethane hydrochloride (Trizma™ HCl; Sigma-Aldrich) and adjusted to pH 7.35.

3.2.2 Electrospinning Process

To prepare polymer solutions containing different concentrations of drugs, PDLLA (10 wt%) was dissolved in chloroform. For each sample, 2 wt% (based on polymer) CTC or TC were pre-dissolved in methanol; for TC drug solutions, samples were prepared at a ratio of methanol: chloroform of 1:16, 1:8, and 1:4, respectively. For CTC drug solutions, the ratio was 1:16, 1:12, 1:8, and 1:4. Polymer-drug solutions were gently stirred at room temperature for at least 12 h. For the electrospinning process, a horizontal experimental setup was used, consisting of a syringe, an 18 gauge needle, an aluminum collecting board, and a high voltage supply. A syringe pump connected to the syringe controlled the flow rate to 1 mL/h. PDLLA/drug mix solution was electrospun at a voltage of 18 kV with a tip-to-collector distance of 15 cm.

3.2.3 Characterization

The morphology of the electrospun fibers was investigated using a Zeiss DMS 940 scanning electron microscope (SEM) at 15 kV. Electrospun mats were sputter-coated

with gold for 2 min to minimize charging effects. The diameters of the fibers were estimated from SEM images.

A DCA-322 (Cahn Instruments) was used to determine the contact angle of electrospun fiber mats to Tris buffer based on the Wilhelmy plate method. Fiber mats were first cut into squares of 10 mm x 10 mm width. To avoid effects caused by fiber swelling, the advancing distance was set to 2 mm with a speed of 80 μm/s and all tests were conducted at room temperature. All tests were done in triplicate and results averaged.

The swelling behavior was evaluated by incubating electrospun mats (20 mm x 20 mm, initial weight W_i) in 20 mL Tris buffer at 37℃ in a thermostated water bath. At each time interval, wet weights of samples (W_s) were measured after gently tapping the sample on filter paper to remove surface water. The degree of swelling (S_w) was calculated as follows:

$$S_w = (W_s - W_i)/W_i$$

All tests were performed in triplicate and the values averaged.

Dried electrospun fibers mats with a thickness of approximately 0.2 mm were weighed and placed into 20 mL Tris buffer, incubated at 37℃ for a specified time interval and shaken at 100 rpm. At every time interval, a fiber mat was removed and placed into 20 mL fresh Tris buffer. Solution absorbance was assayed by a UV-vis spectrophotometer at 368 nm for TC and 377 nm for CTC, and the solution concentration determined from the absorbance standard curves. Each measurement was performed in

triplicate and the values averaged. To determine the actual amount of drug loaded on nano-fibers, a piece of fiber mat was weighed and hydrolyzed in 1 N sodium hydroxide solution, then the solution was diluted and assayed by a UV-vis spectrophotometer. The drug loading efficiency was determined as the actual amount of drug contained in the fiber divided by the original amount of the drug added to the polymer solution. All data were analyzed and fitted by Origin 8.0, OriginLab Corporation.

3.3 Results and Discussion

3.3.1 Morphology of drug-loaded ultrafine fibers

PDLLA ultrafine fibers were electrospun from chloroform with methanol as the co-solvent and loaded with TC or CTC as model antibiotic compounds. Their surface morphology was characterized by scanning electron microscopy (SEM). All electrospun drug-loaded ultrafine PDLLA fibers exhibited a well-formed smooth fibrous structure. None of the samples showed visible micropores on their surface and almost no traces of a bead-and-string structure were observed in any of the samples. Figure 3.1 shows the morphology of fibers containing TC obtained from a methanol-chloroform ratio of 1:8. The appearance of these fibers is representative for the fiber morphology generally observed before and after drug release of all samples prepared from different methanol-chloroform ratios.

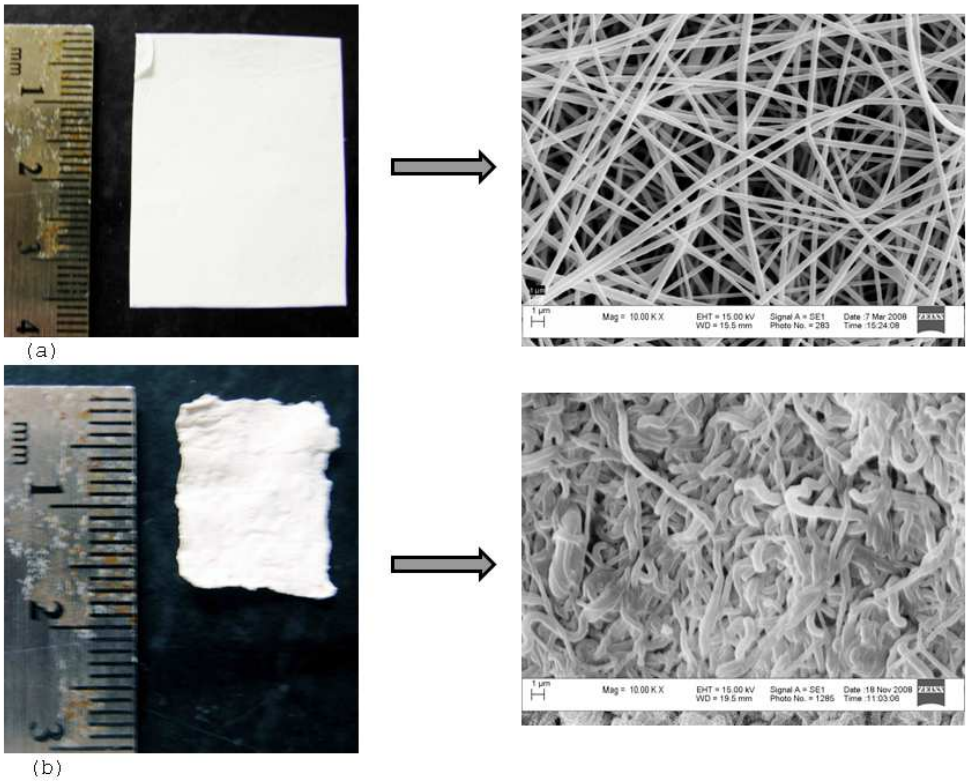

Figure 3.1 Optical (left-hand side) and scanning electron microscopic images (right-hand side) of electrospun TC-loaded PDLLA fibers with a methanol-chloroform ratio of 1:8: (a) directly after electrospinning; (b) after exposure to Tris-buffer for 48 hours.

Average fiber diameters of samples from different systems are listed in Table 3.1. With increasing amount of methanol as co-solvent, the average diameters significantly decreased for all PDLLA systems. In earlier electrospinning studies of Doshi et al,. [6] and Deizel et al,. [25], evidence were presented that the polymer concentration is the dominant factor for the fiber diameter. Most likely, the main reason for the smaller diameter is due to the lower actual concentration of polymer solution with increasing amounts of methanol.

Table 3.1 Average diameters, drug loading efficiency and contact angles of electrospun PDLLA fibers.

Samples	Methanol: chloroform ratio	Diameter (nm)	Drug loading efficiency (%)	Contact angle (°)
PDLLA+ TC	1:16	830±280	62.1±14.65	91.8±0.29
	1:8	360±70	84.1±2.59	92.8±0.91
	1:4	220±60	98.8±0.93	102.2±0.87
PDLLA+ CTC	1:16	1550±330	53.4±18.22	91.7±0.24
	1:12	558±134	88.8±6.49	99.6±2.18
	1:8	515±190	98.9±0.97	101.6±1.01
	1:4	220±50	99.5±2.88	107.9±1.53

In regard to the type of drug incorporated, TC charged fibers showed smaller diameters than CTC loaded fibers. This effect might be the result of higher solubility of TC in methanol, leading to TC's better salt effect, which has a significant influence on the morphology of electrospun fibers [12, 13].

It is important to note that electrospun PDLLA fiber mats showed considerable shrinkage under physiological conditions. As illustrated in Figure 3.1(a), immediately after electrospinning the fibers looked fairly straight, detached from each other and with ample space in-between individual fibers; they evenly overlapped to form a non-woven network structure. Within 120 min in Tris buffer, all PDLLA samples had decreased in size by approximately 70-80% of their original area (Figure 3.1(b)). At a temperature of 37°C, close the glass transition temperature of PDLLA, the nano-fibers appeared bulkier and considerably closer together. As a result, with the elimination of space between the fibers, the size of the non-woven sample was significantly reduced. Similar phenomena had also been observed for membranes made from electrospun poly(lactide-co-glycolide) (PLGA) [26].

3.3.2 Swelling behavior and contact angle of electrospun ultrafine fibers

As shown in Table 3.1, PDLLA fibers loaded with either TC or CTC exhibited hydrophobic properties in Tris buffer with contact angles higher than 90°. It is possible that the hydrophobicity occurred as a consequence of the rough surfaces and the air trapped in-between the nano-fibers [27, 28]. Furthermore, with increasing amounts of methanol added to the electrospinning solution, the contact angle of resultant non-woven fiber mats increased. As discussed above, higher quantities of the co-solvent methanol impacted the average fiber diameter, which lead to more pronounced roughness of the surface of the fiber mats and thus further increased the observed hydrophobic effects.

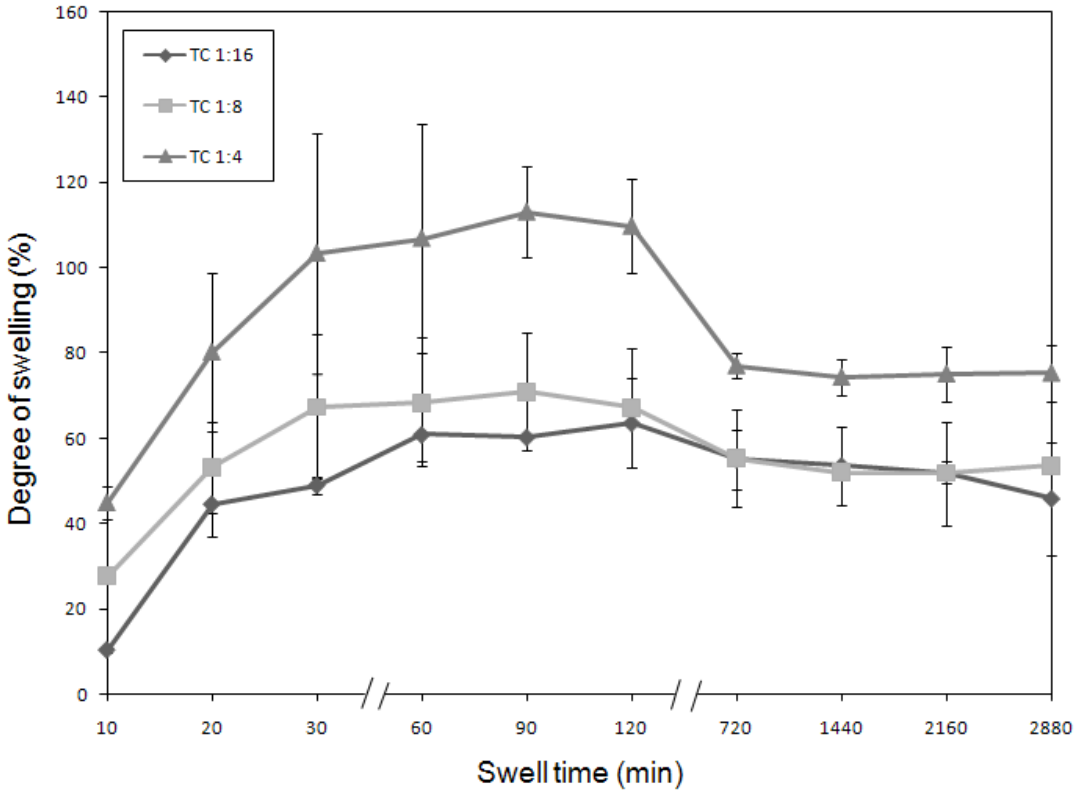

Figure 3.2 Degree of swelling of TC-containing PDLLA fiber mats, prepared at different ratios of methanol:chloroform, in Tris buffer at 37°C.

The swelling behavior of the electrospun drug loaded fibers is shown in Figures 3.2 and 3.3. To the most part, the degree of swelling of the electrospun PDLLA membranes with incorporated drugs increased within 90-120 min. Their swelling tendency can be explained through the contribution of two effects: (1) the swelling caused by the actual liquid pick-up; (2) the hydrophobicity of the membranes. During constant agitation in Tris buffer at 37ºC, the PDLLA mats eventually absorbed water and expelled trapped air. As a result, the weight of the membranes increased. After 90-120 min, the electrospun mats began to become more compact with decreased space between fibers, and subsequently the degree of swelling decreased.

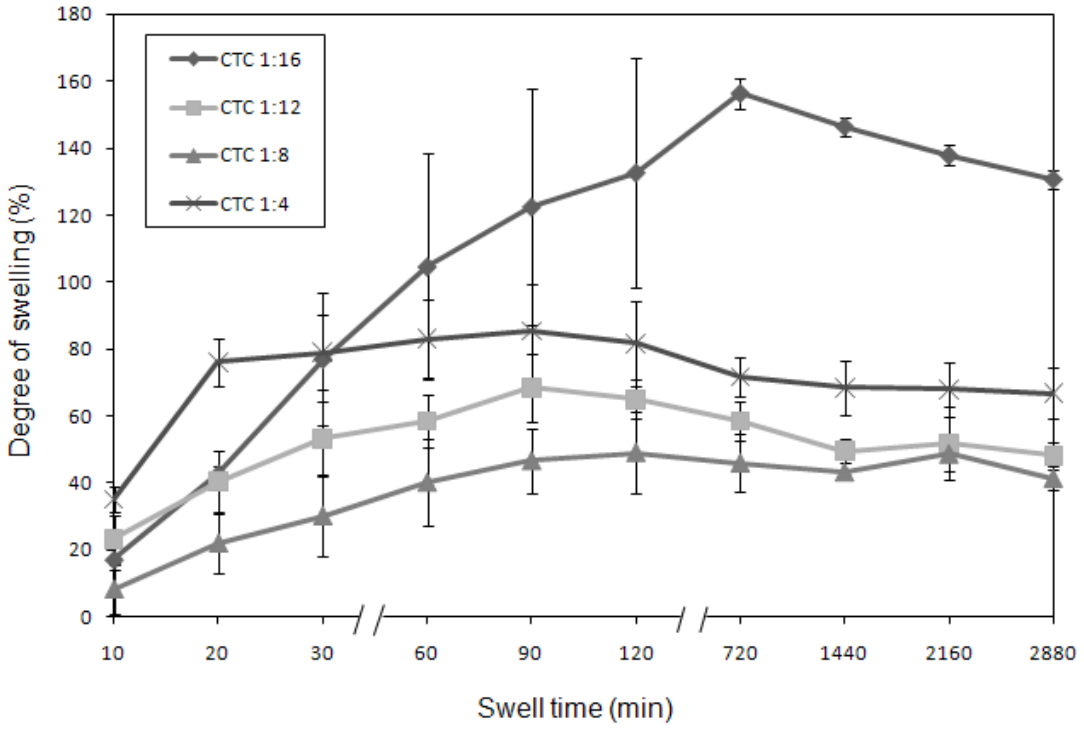

Figure 3.3 Degree of swelling of CTC-loaded PDLLA nano-fibers, prepared at different ratios of methanol:chloroform, in Tris buffer at 37°C.

Differences in swelling were observed depending on whether the membranes contained TC or CTC. For TC loaded PDLLA nano-fibers prepared with higher methanol content, the degree of swelling increased (Figure 3.2). In this case it could be argued that the diameter of the nano-fibers was smaller and thus the space between individual fibers had increased. In contrast, the swelling behavior of CTC loaded nano-fibers proved to be more complicated to explain. When the drug was completely dissolved in the electrospinning solution, a similar trend was observed as for TC samples (e.g., for CTC 1:8 and CTC 1:4 samples). However, in the case of the CTC 1:16 and 1:12 samples, the drug could not be entirely dissolved. Here a significant and increasing amount of sorbed water was measured after a relatively low initial uptake. A possible explanation of this

phenomenon could be that a phase separation between drug and polymer occurred during electrospinning due to the low solubility of CTC under these conditions. An assumption is made that a higher amount of drug molecules is located on the surface of the nano-fibers instead of being encapsulated in the fiber interior due to the polarity of the drugs. Thus, when immersed in buffer solution, drugs on the surface would be flushed out faster than those confined inside and more water might more easily penetrate via channels created by the released drugs. As a consequence, drug/polymer/water interactions would result in a strong increase in swelling of the PDLLA nano-fibers. This assumption was confirmed by drug release experiments (see below).

3.3.3 Drug release studies

The weight of the fiber mats was measured before and after *in vitro* release, and no significant weight loss was observed for any of the samples after 48 h exposure in Tris buffer. Consequently, the effect of polymer hydrolysis and degradation has not been taken into consideration in this study.

Before investigating the drug release profile, the drug loading efficiency was determined. As shown in Table 3.1, the drug loading efficiency of both CTC and TC, as defined as the actual amount of drug divided by the original amount of the drug added to the polymer solution, increased with higher methanol content. All samples except for CTC and TC 1:16 samples actually contained 85-100% of the drug loaded, suggesting that electrospinning could be a sufficiently effective method for encapsulation of drugs. The loading efficiencies of CTC 1:16 and TC 1:16 samples was somewhat lower

compared to the other samples, since very small amounts of solvent were used and traces of the active compound might have been lost due to experimental difficulties, such as the solution transfer and the actual electrospinning process.

The *in vitro* drug release profiles of PDLLA ultrafine fibers are shown in Figures 3.4 and 3.5. Interestingly, CTC and TC drugs exhibited an entirely different release behavior. In the case of fibers containing TC, the rate of drug delivery decreased with higher methanol content. Only approximately 13% were discharged from the TC 1:16 samples while a release of about 33% was observed for TC 1:4 at comparable exposure times (Figure 3.4). In contrast, CTC was released to almost 56% from 1:16 samples and to about 16% from 1:4 samples (Figure 3.5). Overall however, with lower methanol content in the electrospinning solution, CTC was released considerably faster and to a higher extent than TC. It can be speculated that the differences observed in discharge behavior are based on differences in the nature of molecular diffusion of TC and CTC and their solubility in methanol as well as in the release medium (aqueous Tris buffer at pH 7.35).

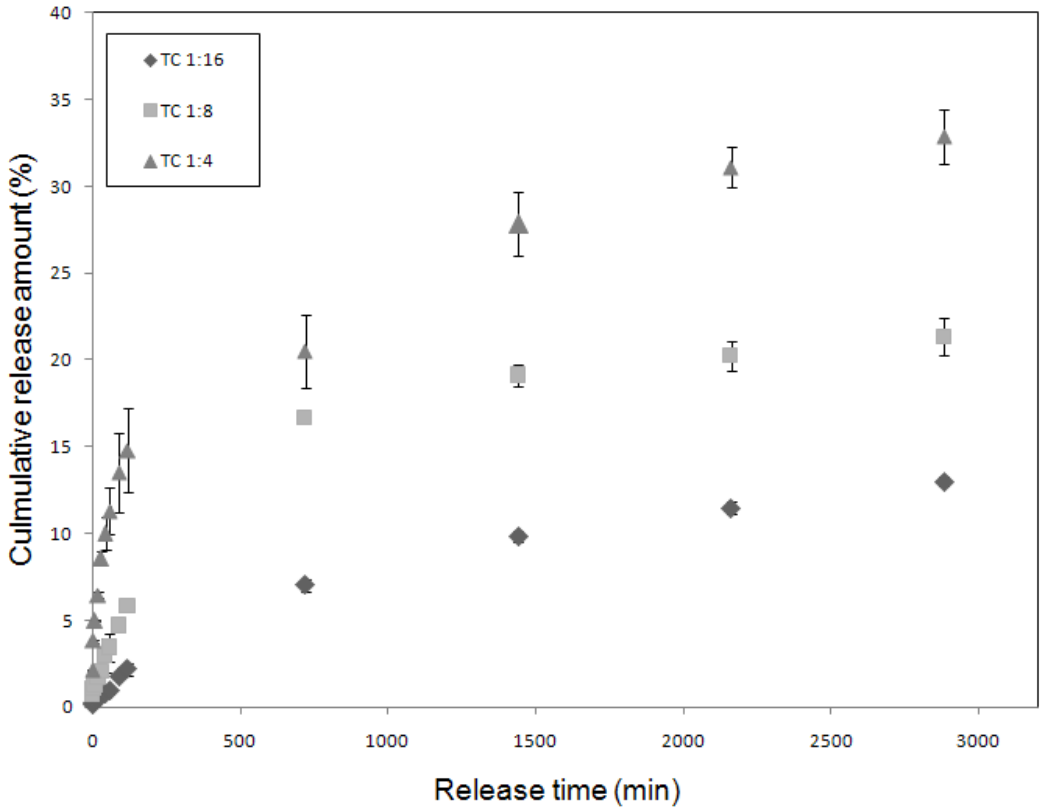

Figure 3.4 TC release from electrospun PDLLA fiber mats into Tris buffer solution at 37°C.

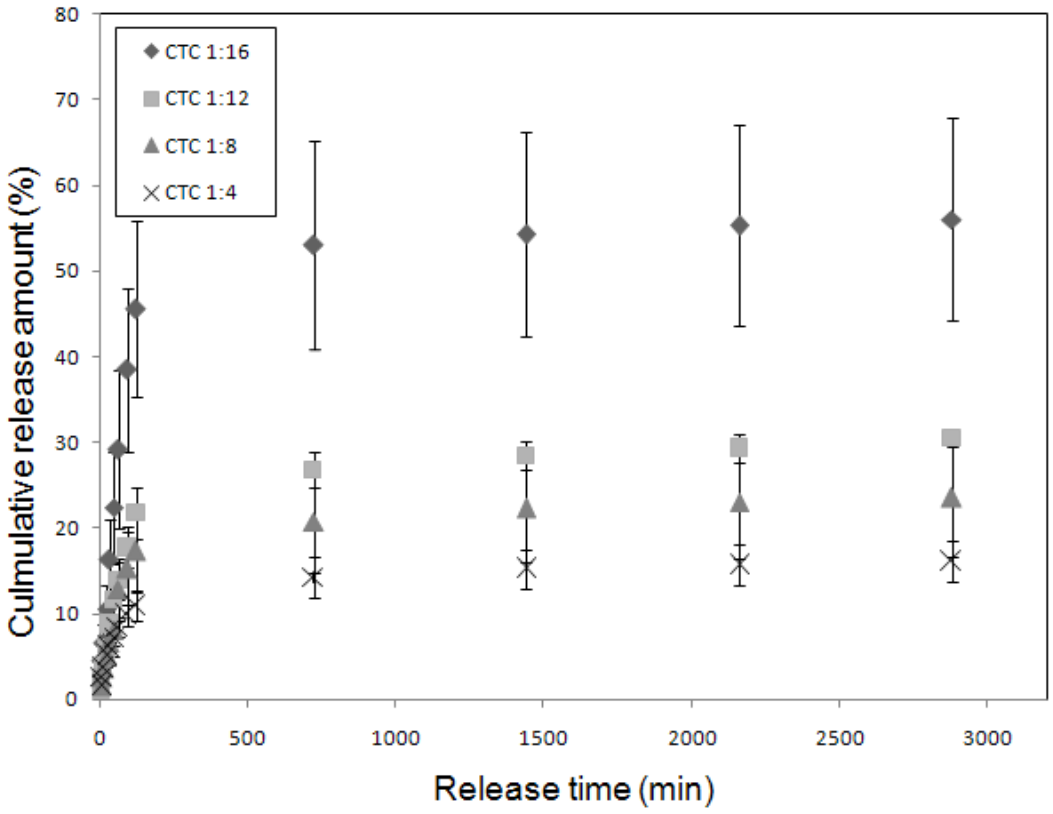

Figure 3.5 CTC release from electrospun PDLLA fiber mats into Tris buffer solution at 37°C.

Srikar [24] suggested a desorption-limited mechanism instead of a diffusion-limited mechanism for drug release from nano-fibers with nanopores on the surface. Since no such nanoporous structure was observed in this study, a diffusion-limited mechanism was assumed. To explain the drug release mechanism from electrospun nano-fibers, the Fickian diffusion model of swellable devices could be applied. According to Ritger and Peppas's research [29], a Fickian diffusional release from a polymer matrix can be described by the following equation,

$$\frac{M_t}{M_\infty} = kt^n \qquad (1)$$

where M_t/M_∞ is the fraction of drug released, k is a constant related to the drug diffusion coefficient, n is the diffusional exponent, which is an indication for the drug release mechanism and t is the drug release time. For TC loaded electrospun PDLLA ultrafine fibers, the drug release data were fitted with eqn. (1) as shown below in eqns. (2) to (4):

TC 1:16, $$\frac{M_t}{M_\infty} = 0.0.133t^{0.665} \qquad r^2 = 0.992 \qquad (2)$$

TC 1:8, $$\frac{M_t}{M_\infty} = 0.0383t^{0.509} \qquad r^2 = 0.984 \qquad (3)$$

TC 1:4, $$\frac{M_t}{M_\infty} = 0.1036t^{0.352} \qquad r^2 = 0.966 \qquad (4)$$

The value of n is depended on the geometry, as indicated by Ritger and Peppas [29], and r^2 is the adjustment coefficient of determination. For example, for Fickian diffusion from a thin film, n is 0.5, while for a cylindrical sample, n is 0.45. Thus, for the case of larger fiber diameters as a result of lower methanol content in the spinning solution, the fiber mesh could be considered a film. On the other hand, at higher concentrations of methanol in the spinning solution and consequently smaller resultant fiber diameters, the electrospun fibers could be regarded as cylinders. However, for the TC 1:16 sample, n is higher than 0.5 because TC might not have been entirely dissolved in methanol and therefore might not have been homogeneously distributed. For the TC 1:4 sample, the deviation of n from 0.45 occurred because the electrospun fibers were not perfectly shaped cylinders and the existence of overlapping and entangled fibers reduced the effective surface for drug release. It was also noticed that k increased with increasing

amount of methanol used, which suggests that with the smaller diameter of the fibers, a higher surface area was available for drug transport and as a consequence, the diffusion coefficient increased.

However, Fickian diffusion did not prove to be a good model for CTC release from PDLLA nano-fibers, as indicated by the lower r^2 values of 0.7 to 0.8. Since CTC is barely soluble in water, it might be more difficult for this drug to diffuse through polymer chains. Here, a Case-II release (non-Fickian diffusion) mechanism was applied to interpret the release behavior. According Ritger [29] and Kosmidis [30], Case-II release is a solute transport based on polymer relaxation, and it can be described as follows,

$$\frac{M_t}{M_\infty} = 1 - \left[1 - \frac{k_0}{C_0 \alpha'} t\right]^N \qquad (5)$$

Here, α' is the diffusional length of the sample and k_0 and C_0 are constants. N is the diffusional exponent, which is determined by sample geometry and ranges from 1 for films, to 2 for cylinders. Initially, the electrospun fibrous membranes were considered as a film. As $N = 1$, the equation can be formulated as shown in (6),

$$\frac{M_t}{M_\infty} = \frac{k_0}{C_0 \alpha'} t \qquad (6)$$

Based on eqn. (6), CTC drug release data were linear-fitted until a saturation value was reached. The linear portion below saturation of each sample can be described as follows,

CTC 1:16, $\frac{M_t}{M_\infty} = 0.3753t$ $r^2 = 0.982$ (7)

CTC 1:12, $\frac{M_t}{M_\infty} = 0.1921t$ $r^2 = 0.958$ (8)

CTC 1:8, $\frac{M_t}{M_\infty} = 0.1380t$ $r^2 = 0.959$ (9)

CTC 1:4, $\frac{M_t}{M_\infty} = 0.0754t$ $r^2 = 0.900$ (10)

It was noticed that the $k_0/C_0\alpha'$ number decreased with increasing amount of methanol used, which is inconsistent with the experimentally observed TC drug release profile. Therefore, polymer chain relaxation seems to be the major driving force of the CTC release from PDLLA fibers. This result is in agreement with data of fiber mat shrinkage and swelling tests of CTC loaded nano-fibers. In the initial phase, the polymer relaxation probably leads to the shrinkage of the membrane. Subsequently, as discussed above, with less methanol used in the electrospinning solution, more drugs may be located on the surface of the electrospun fibers and faster water uptake may occur in these systems. This polymer/drug/water interaction at 37℃ could then have lead to a polymer chain movement that allowed the solution release from the fibrous matrix.

Eqn. (6), however, did not accurately describe the release of CTC from the 1:4 sample, since $r^2 = 0.900$. Analogous to the TC 1:4 sample, CTC 1:4 sample was treated as a cylindrical matrix for drug release, and eqn. (5) with $N = 2$ was applied, leading to eqn. (11),

$$\frac{M_t}{M_\infty} = \frac{2k_0}{C_0\alpha'}t - \left[\frac{k_0}{C_0\alpha'}t\right]^2 \qquad (11)$$

Using a polynomial form to fit CTC 1:4 data,

$$\frac{M_t}{M_\infty} = 0.1505t - 0.00065t^2 + 1.9013 \text{ , } \quad r^2 = 0.984 \qquad (12)$$

However, the parameters in eqn. (12) do not match the requirement of eqn. (11). Thus, the drug release from the CTC 1:4 sample could not simply be described as a Case-II relaxational release. According to Peppas and Sahlin's model [31], eqn. (13) can be formulated:

$$\frac{M_t}{M_\infty} = k_1 t^m + k_2 t^{2m} \qquad (13)$$

On the right-hand side of eqn. (13), the first term is the contribution of Fickian diffusion, while the second term is the contribution of Case-II diffusion and *m* is a geometrical parameter. Considering the CTC 1:4 sample as a cylindrical specimen, *m* is equal to 0.89. Therefore, a non-linear fitting curve could be developed based on

$$\frac{M_t}{M_\infty} = 0.2190t^{0.89} - 0.0005104t^{1.78}, \quad r^2 = 0.959 \qquad (14)$$

Eqn. (14) suggests that with a cylindrical geometric shape, CTC release from the electrospun fibers prepared with a methanol to chloroform ratio of 1:4 was driven by both Fickian and relaxational contributions. The reason is that in this case CTC dissolved very well, which leads to a lower amount of the drug being located on the nanofiber surface. Thus, the influence of Case-II relaxational release was less prominent in CTC 1:4 sample.

3.4 Conclusions

Tetracycline (TC) or chlorotetracycline (CTC) containing ultrafine PDLLA fibers were successfully fabricated by electrospinning. The influence of methanol as a co-solvent in the electrospinning solution was discussed in regard to physical fiber properties and drug release behavior. With increasing amounts of methanol, fiber diameters decreased and contact angle and drug loading efficiency increased. The nano-fiber mats showed considerable area shrinkage and swelling under simulated physiological conditions. Differences in *in vitro* release profiles and swelling behaviors showed that different drug release mechanisms for TC and CTC occurred. A Fickian diffusional release mechanism could be applied to interpret TC drug release from electrospun fibers. However, CTC loaded PDLLA fibers displayed a more complex swelling and release pattern due to the influence of lower drug solubility in the spinning solution and release medium, and as a result of the involved polymer/drug/solvent interactions. In this case, the main driving force of release was proposed to be a Case-II relaxation mechanism for lower methanol ratios and a combination of Fickian diffusion and Case-II mechanism for higher methanol content. The choice of solvent system might therefore be used to control the drug release from nanofibrous materials.

3.5 References

1. Langer, R. Science 1990, 249, 1527.
2. Uhrich, K.E.; Cannizzaro, S.M.; Langer, R.; Shakesheff, K.M. Chemical Reviews 1999, 99, 3181.

3. Mundargi, R.C.; Babu, V.R.; Rangaswamy, V.; Patel, P.; Aminabhavi, T.M. Journal of Controlled Release 2008, 125, 193.

4. Ganta, S.; Devalapally, H.; Shahiwala, A.; Amiji, M. Journal of Controlled Release 2008, 126, 187.

5. LaVan, D.; McGuire, T.; Langer, R. Nature Biotechnology 2003, 21, 1184.

6. Doshi J.; Reneker, D.H. Journal of Electrostatics 1995, 35, 151.

7. Shin, Y.M.; Hohman, M.M.; Brenner, M.P.; Rutledge, G.C. Polymer 2001, 42, 9955.

8. Kidoaki, S.; Kwon, I.K.; Matsuda, T. Biomaterials 2005, 26, 37.

9. Sell, S.; Barnes, C.; Smith, M.; McClure, M.; Madurantakam, P.; Grant, J.; McManus, M.; Bowlin, G.L. Polymer International 2007, 56, 1349.

10. Chen, J.P.; Chang, G.Y.; Chen, J.K. Colloids and Surfaces A: Physicochemical and Engineering Aspects 2008, 313-314, 183.

11. Kenawy, E.R.; Bowlin, G.L.; Mansfield, K.; Layman, J.; Simpson, D.G.; Sanders, E.H.; Wnek, G.E.; Journal of Controlled Release 2002, 81, 57.

12. Zong, X.H.; Kim, K.; Fang, D.F.; Ran, S.F.; Hsiao, B.S.; Chu, B. Polymer 2002, 43, 4403.

13. Kim, K.; Luu, Y.K.; Chang, C.; Fang, D.; Hsiao, B.S.; Chu, B.; Hadjiargyrou, M. Journal of Controlled Release 2004, 98, 47.

14. Huang, Z.M.; He, C.L.; Yang, A.Z.; Zhang, Y.Z.; Han, X.J.; Yin, J.L.; Wu, Q.S. Journal of Biomedical Materials Research Part A 2006, 77A, 169.

15. Liao, I.C.; Chew, S.Y.; Leong, K.W. Nanomedicine 2006, 1, 465.

16. Chunder, A.; Sarkar, S.; Yu, Y.B.; Zhai, L. Colloids and Surfaces B:

Biointerfaces 2007, 58, 172-179

17. Chew, S.Y.; Wen, J.; Yim, E.K.F.; Leong, K.W. Biomacromolecules 2005, 6, 2017.

18. Zeng, J.; Aigner, A.; Czubayko, F.; Kissel, T.; Wendorff, J.H.; Greiner, A. Biomacromolecules 2005, 6, 1484-1488

19. Peng, H.S.; Zhou, S.B.; Gou, T.; Li, Y.S.; Li, X.H.; Wang, J.X.; Weng, J. Colloids and Surfaces B: Biointerfaces 2008, 66, 206.

20. Kenawy, E.R.; Abdel-Hey, F.I.; El-Newehy, M.H.; Wnek, G.E. Materials Chemistry and Physics 2009, 113, 296.

21. Xie J.W.; Wang, C.H. Pharmaceutical Research 2006, 23, 1817.

22. Zeng, J.; Yang, L.X.; Liang, Q.Z.; Zhang, X.F.; Guan, H.L.; Xu, X.L.; Chen, X.S.; Jing, X.B. Journal of Controlled Release 2005, 105, 43.

23. Taepaiboon, P.; Rungsardthong, U.; Supaphol, P. Nanotechnology 2006, 17, 2317.

24. Srikar, R.; Yarin, A.L.; Megaridis, C.M.; Bazilevsky, A.V.; Kelley, E. Langmuir 2008, 24, 965.

25. Deitzel, J.M.; Kleinmeyer, J.; Harris, D.; Tan, N.C.B. Polymer 2001, 42, 261.

26. Jiang, H.L.; Fang, D.F.; Hsiao, B.; Chu, B.; Chen, W.L. Journal of Biomaterials Science Polymer Edition 2004, 15, 279.

27. Ma, M.L.; Hill, R.M.; Lowery, J.L.; Fridrikh, S.V.; Rutledge, G.C. Langmuir 2005, 21, 5549.

28. Zhu, M.F.; Zuo, W.W.; Yu, H.; Yang, W.; Chen, Y.M. Journal of Materials Science 2006, 41, 3793.

29. Ritger P.L.; Peppas, N. A. Journal of Controlled Release 1987, 5, 37.

30. Kosmidis, K.; Rinaki, E.; Argyrakis, P.; Macheras, P. International Journal of Pharmaceutics 2003, 254, 183.

31. Peppas N.A.; Sahlin, J.J. International Journal of Pharmaceutics 1989, 57, 169.

CHAPTER 4 FUNCTIONALIZED POLY(L-LACTIDE) NANOPARTICLES FROM ELECTROSPUN NANOFIBERS

4.1 Introduction

In the past several years, nanoparticles and nanocrystals have been studied intensively for drug delivery, bioassay and bioimaging applications [1, 2]. It has been demonstrated that both nanoparticles and nanocrystals can help to improve the blood circulation time and site-specific targeting if used for controlled release drug delivery [3, 4]. Until now, several different techniques have been explored to form polymeric nanoparticles, for example, liposome formation [5], self-assembly of amphiphilic polymers [6], layer-by-layer assembly [7] and template-based particle fabrication [8]. Most of these techniques are based on a "bottom-up" routine. As an alternative, a "top-down" routine presents another significant approach for nanoparticle preparation [9]. Recently, fluorescently labeled cellulose nanocrystals have been fabricated as bio-diagnostic agents by degradation of cellulose micro-fibers [10]. This approach was the inspiration for the novel methodology presented here - to create polymeric nanoparticles from micro- or nanofibers.

The size and morphology of the nanoparticles have a significant impact on their interactions with cells. It was found by several research groups that particles with

dimensions of sub-micron to several microns in size can be efficiently attached to cells [13, 14]. Lorenz et al,. [15] reported that fluorescent-labeled polymeric particles with diameters from 168 nm to 1290 nm had been taken up by a variety of cell lines. Although nanoparticles used for biomedical applications frequently are smooth, surface roughness and porous structure does not seem to have a negative impact on cells as demonstrated by a number of research studies [16-18]. On the contrary, nano-scale surface features could actually help cell adhesion and proliferation.

In the past decade, electrospinning has proved to be an easy, effective and versatile technique to fabricate a variety of nanomaterials [19, 20], not only to produce non-woven nanofibrous mats, but also to create a wide range of novel nano-structures for specific applications; for example, core-shell nanofibers [21], well-aligned continuous nanofibers [22] and nano-composites [23]. Functionalization of and drug delivery from electrospun nanofibers has been the target of numerous studies in the biomedical field [24, 25]. Most recently, short fibers with ultrathin diameters became a new application for electrospinning. Kim et al,. [26] used an aminolysis method to breakdown electrospun nanofibers with the goal of preparing nanocylinder fragments. Short electrospun fibers with a length of 20-30μm to 100-150 μm could also be prepared by a UV cutting method [27].

In this chapter, electrospun nanofibers from poly(L-lactide) (PLLA) were employed as a template to create crystalline nanoparticles with controllable size via a “top-down” method. The dimensions and morphology of the particles were assessed by light scattering particle size analysis and scanning electron microscopy (SEM). Differential

scanning calorimetry (DSC) and wide angle x-ray diffraction (WAXD) was conducted to obtain information on the crystal formation of the samples. The PLLA nanocrystals were successfully labeled with fluorescein-5'-isothiocyanate (FITC) as a fluorescent agent by the reaction between the isothiocyanate group and the amine groups on the surface of the nanocrystals. It was possible to show that this is an easy, controllable routine to generate crystalline polymer nanoparticles for potential delivery of therapeutics.

4.2 Experimental Section

4.2.1 Materials

Poly(L-lactide) (PLLA) with a molecular weight of 85,000 to 160,000 Daltons was purchased from Sigma-Aldrich. Fluorescein-5'-isothiocyanate (FITC), benzyltriethylammonium chloride (BTEAC), and 1, 6-hexanediamine were also obtained from Sigma-Aldrich. All solvents were of analytical grade and purchased from Fisher Scientific.

4.2.2 Electrospinning

To prepare nanofibers, PLLA was dissolved in chloroform with concentrations varying from 3 to 10 wt%. To each solution 10 mg BTEAC were added to facilitate the electrospinning process. A horizontal experimental setup was used, consisting of a syringe, an 18 gauge needle, an aluminum collecting board, and a high voltage supply. A

syringe pump, connected to the syringe, controlled the flow rate to 1 mL/h. PLLA solution was electrospun at a voltage of 18 kV with a tip-to-collector distance of 15 cm.

4.2.3 Aminolysis and FITC labeling

Nanofibrous mats obtained by electrospinning were dried overnight, and subsequently immersed in 10% 1,6-hexanediamine/2-propanol solution at 42˚C with shaking at 120 rpm for reaction times varying from 4 to 10 h. The chemical reaction of aminolysis was illustrated in Scheme 4.1. The suspension was then centrifuged, thoroughly washed with DI water, sonicated for 1 min, and freeze-dried. The yield was determined quantitatively. Fluorescein-5'-isothiocyanate (FITC) was covalently bound to the obtained PLLA nanoparticles in a methanol-water mixture at a ratio of 3:1 by overnight stirring at room temperature in the dark. The remaining unreacted FITC was removed by dialysis against 10 mM phosphate buffered saline until no more dye was released. The absorbance of the nanoparticle suspension before and after FITC labeling was characterized by UV-vis spectrometry.

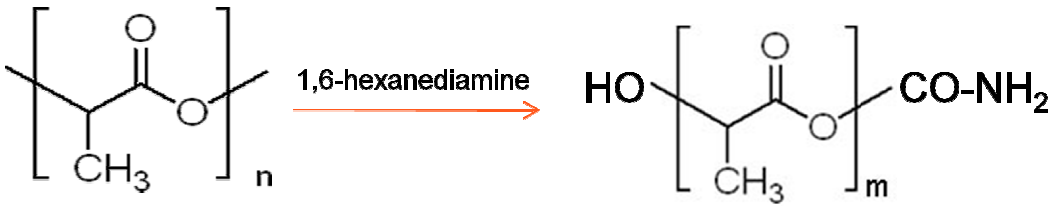

Scheme 4.1 The chemical reaction of aminolysis

4.2.4 Characterization

The particle size was assessed by use of a NICOMP TM 380 ZLS Particle Sizing System at a scattering angle of 90°. The data was processed by the software of ZPW388 v1.89 with NICOMP analysis method. For SEM images, 25 μL of the suspension were placed on a silicon wafer, which was attached to an aluminum stub by carbon tape. The nanofiber and nanoparticle samples were sputter-coated with gold and characterized by a Zeiss DMS 940 SEM at 15 kV.

To determine the thermal properties, samples were first lyophilized by freeze-drying, followed by thermal analysis with a differential scanning calorimeter (DSC, TA Instrument Q2000) at a ramp rate of 10˚C/min. The crystalline structure of PLLA nanoparticles was characterized by using a Bruker D8 X-ray diffactometer at 40 kV, 40 mA (CuKα radiation with a wavelength of 1.54 Å), 2θ range from 5 to 30˚ at intervals of 0.01˚.

After labeling with FITC, the PLLA nanoparticles were sonicated for 30 s, the pH of the suspension was adjusted to 11 and the amount of FITC on the nanocrystals quantified by determining the absorbance at 490 nm via UV-vis spectroscopy. A calibration curve was prepared with free FITC in ammonium hydroxide solution at pH 11.

4.3 Results and Discussion

The morphology of typical PLLA fibers, electrospun from 10wt% PLLA solution in chloroform, is shown in Figure 4.1a. The fibers, with a smooth surface (Figure 4.1b), were uniform in width with an average fiber diameter of 700 nm. After aminolysis, the fibers were reduced to short nanoparticles with roughly rectangular shape (Figure 4.1c; 6

h aminolysis; Figure 4.1d; 10 h aminolysis). A close examination of the particles revealed that their surface was now no longer smooth (Figure 4.1e), but appeared to be rather “rugged”. Kim and Park [26] reported a similar morphology in their study. They argue that the reason for the formation of an uneven surface might be found in a competing mechanism of PLLA chain degradation and simultaneous recrystallization of the shortened chains.

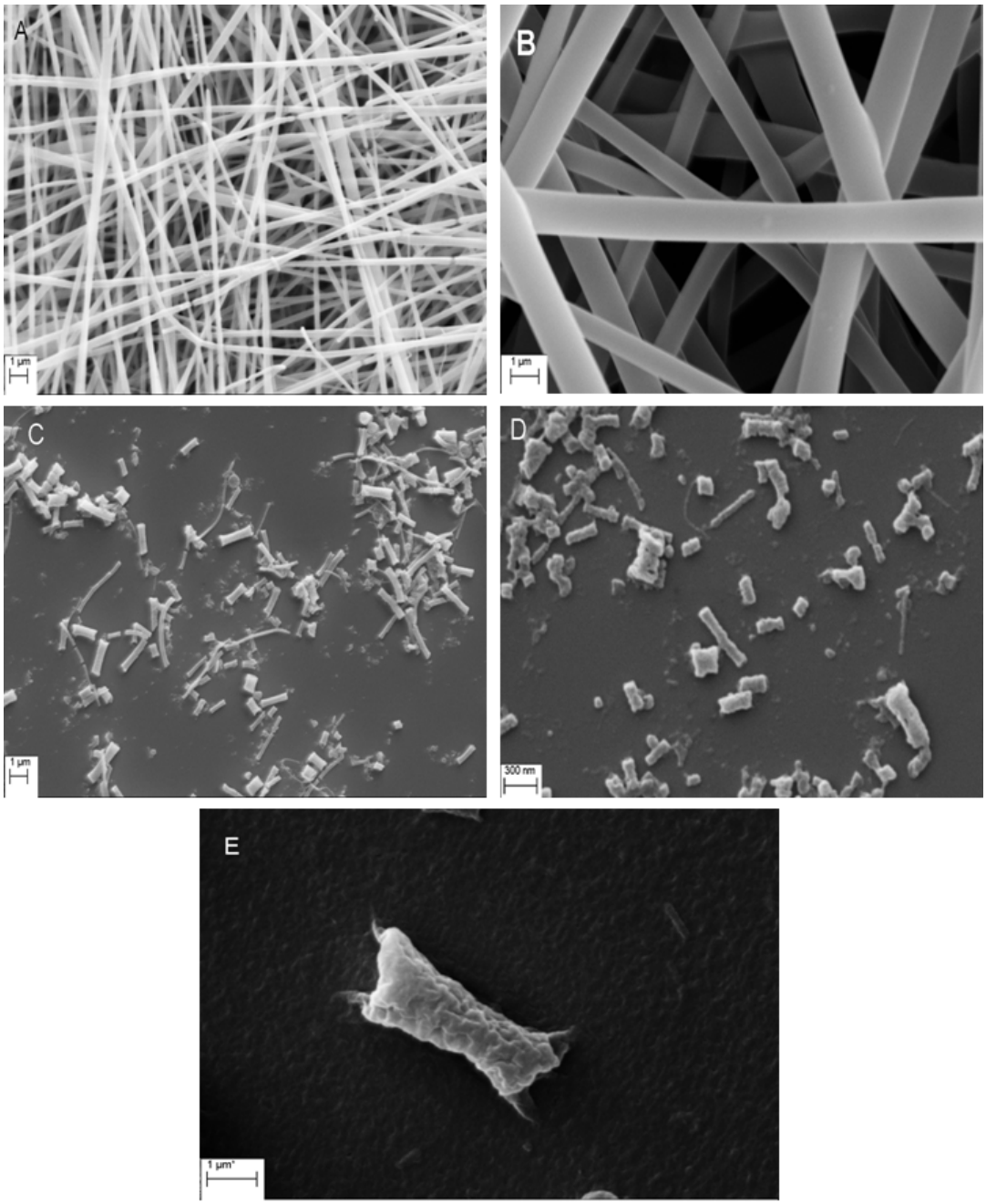

Figure 4.1 SEM images of (A) electrospun 10wt% PLLA nanofibers; (B) enlarged image of PLLA nanofibers; (C)PLLA nanoparticles from electrospun 10wt% PLLA nanofibers after 6 h aminolysis; (D) PLLA nanoparticles from electrospun 10wt% PLLA nanofibers after 10 h aminolysis. (E) enlarged image of PLLA nanoparticles in (C);

The size and surface morphology of the particles play an important role for their suitability in biomedical applications. The average dimensions and the distribution of the particles were characterized by a light scattering particle size analyzer; length and diameter of the particles were determined from SEM images. The influence of aminolysis time was found to have a significant impact on particle size. In Figure 4.2, a typical example of this dependency is illustrated for electrospun fibers obtained from 5wt% PLLA solution. With longer aminolysis time, the size of the PLLA particles became noticeably smaller. For instance, after 4 h aminolysis, the generated average particle size was about 470 nm, while after 10 h degradation, the average particle size decreased by more than half to only 220 nm. In Table 4.1, typical data are presented for various electrospinning solution concentrations and aminolysis times. As expected, with longer aminolysis time, the size of the PLLA particles became noticeably smaller. For instance, after 4 h aminolysis, the aspect ratio of the generated average particle was 5.3, while after 10 h degradation the aspect ratio dropped to 1.7. Unfortunately, longer aminolysis time also significantly reduced the yield of PLLA nanoparticles.For instance, to prepare nanoparticles of 220 nm with 10 h aminolysis, the yield was less than 5%. As a consequence, the method had to be modified to improve the yield.

It is well-known that the diameters of electrospun fibers can be easily controlled by altering the concentration or composition of the spinning solution [28]. Therefore, to produce small particles at high yield, PLLA nanofibers were prepared with smaller diameters, which were then aminolyzed for a shorter time period. As shown in Figure 4.3 and Table 4.1, electrospun fiber diameters decreased when made from lower PLLA solution concentration. Fibers electrospun from 10 wt% PLLA and 6 h aminolysis

produced fairly large particles with aspect ratio of 3.8 at a yield of 57.8%, while electrospun from a 3 wt% solution and aminolyzed for 6 h yielded nanoparticles with an aspect ratio of 2.8 at a yield of over 30%. The average particle size as measured by light scattering was 279 nm under these conditions and thus slightly larger than for 5 wt% solution and 10 h aminolysis (216 nm). However, the yield was clearly improved. With this alternative experimental approach, the particles were slightly larger than the diameter of the electrospun nanofibers from which they originated, suggesting that the shape of the prepared nanoparticles is cylindrical with the length being larger than the fiber diameter.

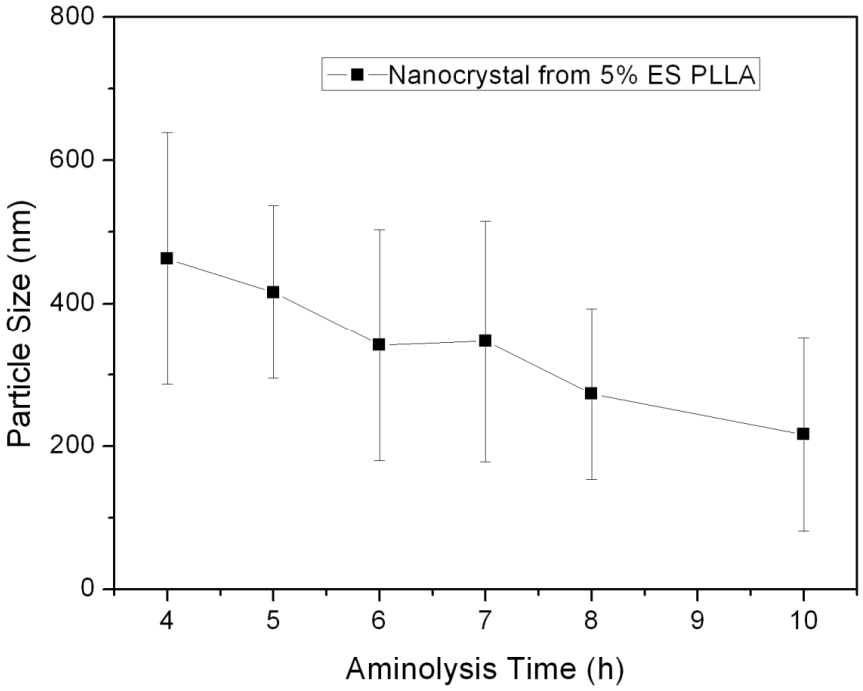

Figure 4.2 Influence of the duration of the aminolysis reaction on the size of the resulting PLLA particles (ES = electrospun).

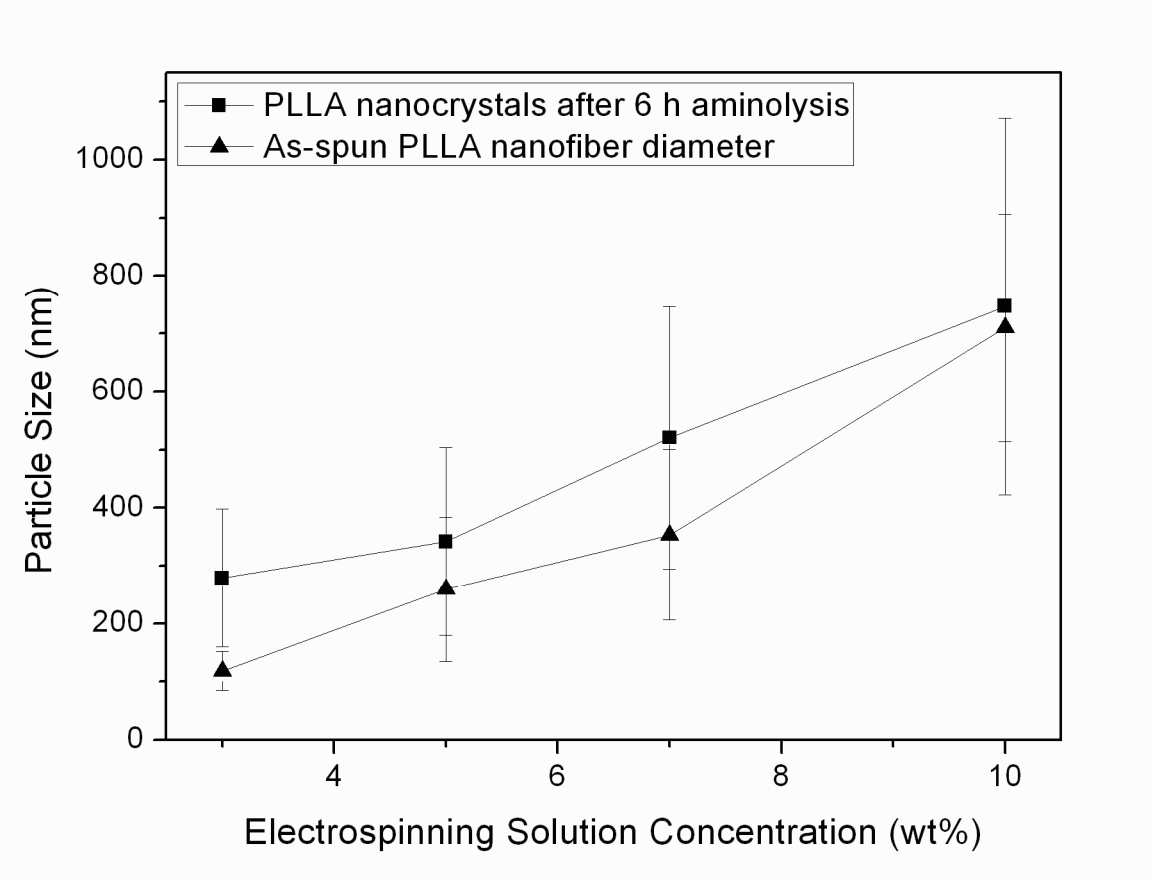

Figure 4.3 Influence of PLLA solution concentration on nanofiber diameter, and in turn, on the size of the resulting nanoparticles.

Kim and Park [26] indicated that electrospun PLLA showed transverse fragmented crystalline structure after aminolysis. Thus, the nanoparticles made by this method were investigated by wide angle x-ray diffraction (WAXD). As can be seen in Figure 4.4, the particles were highly crystalline. The x-ray diffraction patterns presented were obtained from particles originated from electrospun PLLA fibers of 5wt% solution as an example. Directly after electrospinning fibers were purely amorphous as the amorphous scatter in the x-ray spectrum indicated. It has to be considered that the electrospinning process is extremely fast, leaving little time for crystallization. In addition, PLLA polymer chains

do not readily crystallize [29]. However after aminolysis, the PLLA nanoparticles clearly exhibited a crystalline diffraction pattern as usually observed for the α-form of PLLA (Figure 4.4). The strongest reflection was located at 2θ = 16.9° due to the diffraction from the (200) and/or (110) faces. Furthermore, a strong reflection at 2θ = 19.1° was noticed which might stem from (203) faces [30].

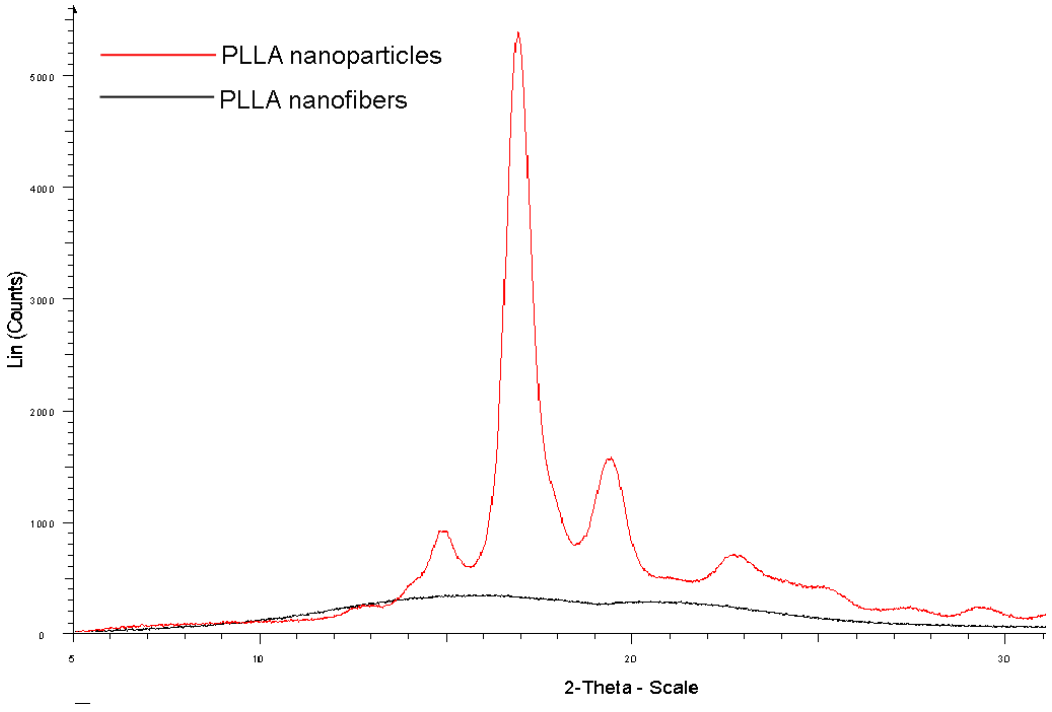

Figure 4.4 Wide angle x-ray diffraction of electrospun PLLA before and after aminolysis.

To further investigate the structure of the PLLA nanoparticles, DSC experiments were conducted for samples produced at different lengths of time of aminolysis (Figure 4.5) and at different electrospinning solution concentrations (Figure 4.6). As exhibited by Figure 4.5, electrospun PLLA showed a clear glass transition temperature (T_g) at 52˚C and a crystallization peak (T_c) at about 75˚C. Also, nanofibersPLLA nanoparticles

obtained after 4 h of aminolysis still exhibited same peaks. However, after 6 to 8 h aminolysis, the crystalline regions became more dominant in the PLLA fragments, as the T_g gradually became hard to observe. The melting temperature (T_m) peak shifted towards lower temperatures from approximately 171 (4 h aminolysis) to 136˚C with longer aminolysis time, suggesting that the molecular weight decreased. Interestingly though, the diameter of the original nanofiber and the duration of the aminolysis reaction seemed to have a similar impact on Tg, Tc and the crystallinity as illustrated in Figure 4.6.

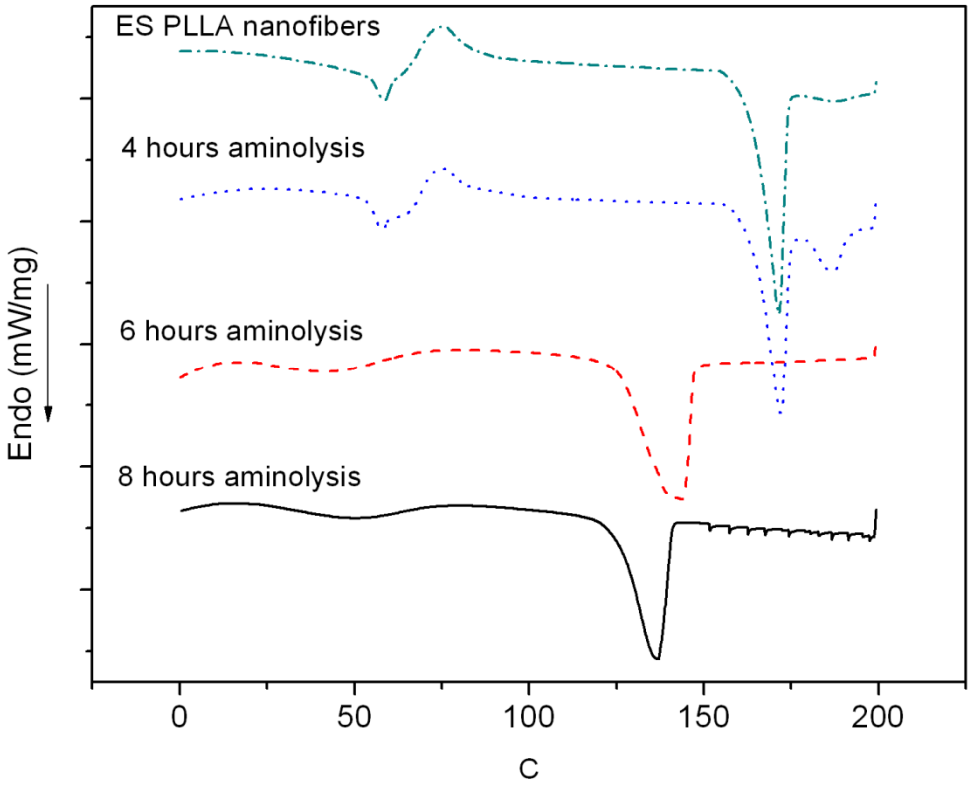

Figure 4.5 DSC of PLLA nanoparticles prepared by varying the duration of the aminolysis reaction. All samples were based on electrospun 7% PLLA (ES = electrospun).

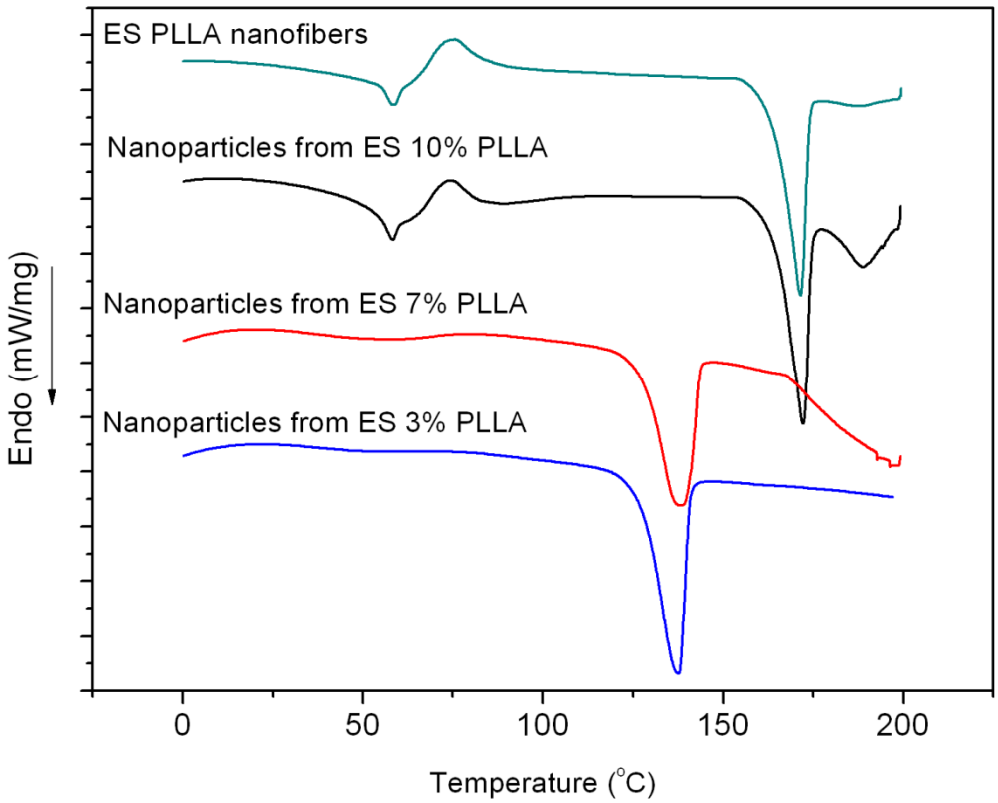

Figure 4.6 DSC of PLLA nanoparticles prepared from different electrospinning solution concentrations (ES = electrospun) with 6 h aminolysis.

As indicated by Table 4.1, the molecular weight as determined by GPC measurements decreased with longer aminolysis time. The original number average molecular weight (Mn) of as-spun 5% PLLA was determined to 104,160 Da with a polydisperse index (PDI) of 1.13. After 4 h aminolysis, the Mn decreased to 7529 Da. With the progressing degradation, the Mn continued to drop to 6861, 5952, and 5246 Da for 6, 8, and 10 h aminolysis, respectively. However, the molecular weights of PLLA nanoparticles made from electrospun nanofibers with different diameters remained almost the same after a set period of aminolysis. For samples from electrospun 3%, 5%, 7%

and 10% PLLA, the Mn were 6202, 6861, 6525 and 6209 Da, respectively. Thus, the reaction time of aminolysis seems to be the decisive factor for the molecular weight of the polymers that constitute the nanoparticles.

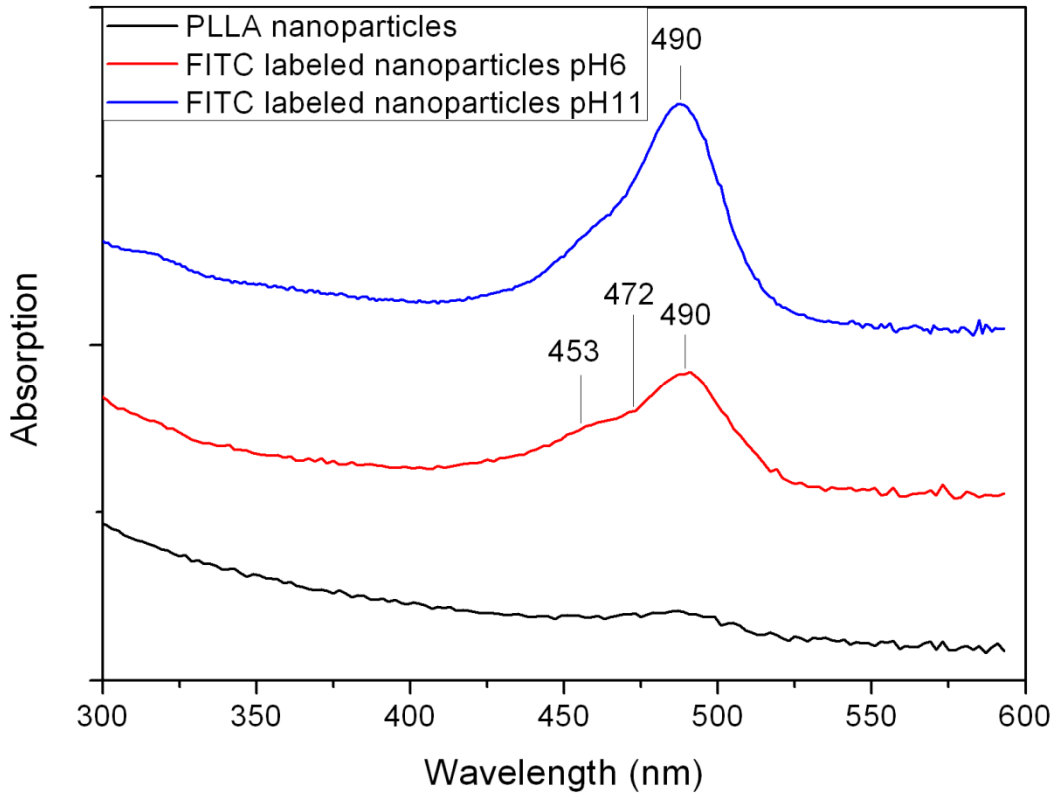

Figure 4.7 UV-vis spectrum of PLLA nanoparticles suspension before and after FITC labeling.

An added benefit of this method to prepare PLLA nanoparticles is that amine groups are generated on the surface of the nanoparticles after the reaction with 1,6 hexanediamine, which are available for further modification. For this research, a fluorescent dye, fluorescein-5'-isothiocyanate (FITC), was bound to the PLLA nanoparticles through the reaction of the isothiocyanate and the amine groups. The

aqueous suspension of PLLA nanoparticles directly after aminolysis was white and opaque; after FITC binding it appeared yellow-green in color.

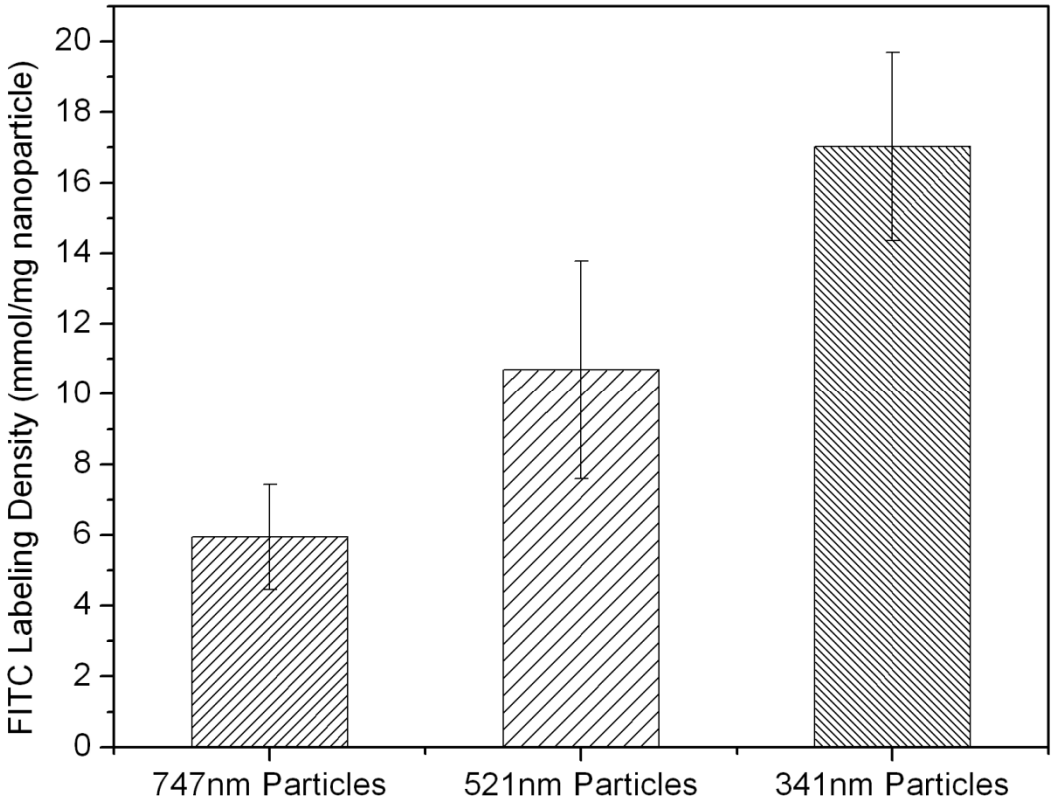

Figure 4.8 Density of binding sites for FITC on the surface of PLLA nanoparticles of different size.

The FITC-labeled PLLA nanoparticles were characterized by UV-vis spectroscopy at different pH-values of the suspension (Figure 4.7). Without fluorescent labeling, PLLA nanoparticles showed no absorption peak. At pH 6, three absorption peaks were observed for the labeled sample. The peak at 490 nm corresponds to the dianionic form, while peaks at 472 and 453 nm originate from the anionic form of FITC [31]. At pH 11, only

the dianionic form exists and shows a peak at 490 nm. This peak was also observed for the free FITC in ammonium hydroxide solution.

Table 4.1 Average size, length, and diameter of PLLA nanoparticles formed in relationship to different aminolysis time and concentration of electrospinning solution. Average molecular weights (Mn) and polydispersity index (PDI) were obtained by GPC measurements.

Solution concentration (wt%)	Aminolysis time (h)	Average size (nm)[a]	Length (nm)[b]	Diameter (nm)[b]	M_n (Dalton)	PDI	Surface Area (μm^2)[c]
5	4	462±176	2581±1015	491±206	7529	1.41	9.48
5	6	341±162	1027±413	273±32	6861	1.41	2.23
5	8	273±120	499±237	225±86	5952	1.29	1.02
5	10	216±135	293±131	177±64	5246	1.20	0.52
3	6	279±119	441±255	155±46	6202	1.39	0.58
5	6	341±162	1027±413	273±32	6861	1.41	2.23
7	6	521±226	1112±526	329±144	6525	1.43	2.98
10	6	747±325	2515±717	669±235	6209	1.37	13.38

a Data from light scattering particle size analysis. b Data from measurement of SEM images. c Assuming particles in the shape of cylinders; dimensions calculated from on SEM measurements.

The particle size certainly plays an important role for the absorbance of the suspensions. The smaller the particles are, the larger is the surface area overall and the more accessible surface functional groups can be expected. As shown by UV-vis

spectroscopy (data not included), the main peak at 490 nm only differed in intensity, but not in position which indicates that no color shift occurred, and thus the PLLA-dye interaction did not change. The graph presented in Figure 4.8 clearly illustrates the difference observed for nanoparticles prepared from 10%, 7% and 5% polymer solution with a corresponding particle size of 750, 420, 340 nm, respectively. After the pH was adjusted to 11, all FITC was in dianionic form. It could be demonstrated that with smaller particles the amount of FITC fixed to the surface of the nanocrystals was noticeably higher due to increased surface area and accordlingly, more amine groups on the surface. Assuming that the nanoparticles are in the shape of a cylinder, the density of PLLA would be 1.27 g/cm^3 [32]. Neglecting the top and bottom surface area of the cylinder, the surface density of binding sites for FITC is 0.015, 0.048, 0.095 moieties per nm^2 for 750, 429, 340 nm PLLA nanoparticles, or one FITC molecule per 67, 21, 11 nm^2, respectively.

4.4 Conclusion

In this study, a “top-down” method was applied to prepare PLLA nanoparticles via electrospinning and aminolysis. The size of nanoparticles was controlled by changing aminolysis time or, more effectively, the diameter of the electrospun fibers. The nanoparticles were generated by both the breakdown of amorphous regions and recrystallization of degraded PLLA. As revealed by WAXD and DSC tests, a higher amount of crystalline regions existed in form of the typical α-crystal modification of PLLA while the molecular weight decreased in the nanoparticles with decreasing particle size. After aminolysis, amine groups were created on the surface of PLLA nanoparticles.

These functional groups are available for further reactions with pharmaceuticals, biomolecules or other compounds. In this study FITC, a fluorescent dye, was employed to demonstrate the potential of the created functional groups. Simultaneously, FITC was also used to show the available surface area of the formed particles for further reaction. As expected, the amount of bound FITC could be correlated to the available surface area of nanoparticles. In summary, with this novel approach it was possible to prepare PLLA nanoparticles of specific controllable size and with surface groups that could be used to anchor biologically useful substances for future drug delivery, biosensors, or bio-imaging applications.

4.5 References

1. Soppimath K.S.; Aminabhavi T.M.; Kulkarni A.R.; Rudzinski W.E. J. of Controlled Release 2001, 70, 1.
2. Rosi N.L.; Mirkin C.A. Chem. Rev. 2005, 105, 1547.
3. Vonarbourg A.; Passirani C.; Saulnier P.; Benoit J-P. Biomaterials 2006, 27, 4356.
4. Moghimi S.M.; Hunter A.C.; Murry J.C. Pharm. Rev. 2001, 53, 283.
5. Lian T.; Ho R.J. J. of Pharm. Sci. 2001, 90, 667.
6. Murthy K.S.; Ma Q.; Clark C.G.; Remsen E.E.; Worley K.L. Chem. Commun. 2001, 773.
7. Kim B.S.; Park S.W.; Hammond P.T. ACS Nano 2008, 2, 386.
8. Gratton S.E.; Napier M.E.; Ropp P.A.; Tian S.; DeSimone J.M. Pharm. Res. 2008, 25, 2845.

9. Wang D.; Möhwald H. J. of Mater. Chem. 2004, 14, 459.

10. Dong S.; Roman M. J. Am. Chem. Soc. 2007, 129, 13810.

11. D. Wang and H. Möhwald, J. of Mater. Chem. 14, 459 (2004).

12. S. Dong and M. Roman, J. Am. Chem. Soc. 129, 13810 (2007).

13. M.P. Desai, V. Labhasetwar, E. Walter, R.J. Levy and G.L. Amidon, Parma. Res. 14, 1568 (1997).

14. M.P. Desai, V. Labhasetwar, G.L. Amidon and R.J. Levy, Parma. Res. 13, 1838 (1996).

15. M.R. Lorenz, V. Holzapfel, A. Musyanovych, K. Nothelfer, P. Walther, H. Frank, K. Landfester, H. Schrenzenmeier and V. Mailänder, Biomaterials 27, 2820 (2006).

16. Y. Hong, C. Gao, Y. Xie, Y. Gong, J.Shen, Biomaterials 26, 6305 (2005).

17. L. Lao, H. Tan, Y. Wang, C. Gao, Colloids & Surfaces B: Biointerfaces 66, 218 (2008).

18. J. Carpenter, D. Khang, T.J. Webster, Nanotechnol. 19, 505103 (2008).

19. Sill T.J.; von Recum H.A. Biomaterials 2008, 29, 1989.

20. Greiner A.; Wendoff J.H. Angew. Chem. Int. Ed. 2007, 46, 5670.

21. Reznik S.N.; Yarin A.L.; Zussman E.; Bercovici L. Phys. Fluids 2006, 18, 062101.

22. Li D.; Wang Y.; Xia Y. Adv. Mater. 2004, 16, 361.

23. Hou H.; Reneker D.H. Adv. Mater. 2004, 16, 69.

24. Xie Z.W.; G. Buschle-Diller J. Appl. Polym. Sci. 2010, 115, 1.

25. Buschle-Diller G.; Cooper G.; Xie Z.W.; Wu Y.; Waldrup J.; Ren X.H. Cellulose 2007, 14, 553.

26. Kim T.G.; Park T.G. Macromol. Rapid. Commun. 2008, 29, 1231.

27. Stoiljkovic A.; Agarwal S. Macromol. Mater. and Eng. 2008, 293, 895.

28. Zong X.; Kim K.; Fang D.; Ran S.; Hsiao B.S.; Chu B. Polymer 2002, 43, 4403.

29. Inai R.; Kotaki M.; Ramakrishna S. Nanotechnology 2005, 16, 208.

30. Cho J.; Baratian S.; Kim J.; Yeh F.; Hsiao B.S.; Hunt J. Polymer 2003, 44, 711.

31. Sjöback R.; Nygren J.; Kubista M. Spectrochim Acta Part A 1995, 51, L7.

32. Lao L.; Tan H.; Wang Y.; Gao C. Colloids Surf. B: Biointerfaces 2008, 66, 218.

CHAPTER 5 SURFACE ENTRAPMENT MODIFICATION OF ELECTROSPUN POLY(D, L)-LACTIDE MATS FOR TISSUE ENGINEERING

5.1 Introduction

In recent years, electrospinning has been studied intensively as an easy, effective and versatile technique to fabricate nonwoven materials with fiber diameters in the range of a few nanometers to several microns [1, 2]. Ultra-fine polymer fibers from almost any kind of polymer solution can be produced by using the electrostatic force between a needle spinneret and a grounded collector [3, 4]. Electrospun nonwoven mats with a very large surface area to volume ratio have been developed targeting a wide range of applications, such as filters [5], catalysts [6], sensors [7], and especially biomedical materials in tissue engineering, wound healing and drug release [8-10].

For any practical applications of electrospun nanofibers, surface properties are most important. Especially for biomedical materials, surface properties are critical to get the desired biological interactions [11, 12]. Surface modifications can be approached during electrospinning process by design of the set-up [13, 14], or after electrospinning. Post-spin chemical modification is the major method studied by researchers, and hydrolysis [15], air plasma treatment [16, 17], and surface grafting [18] have been reported. Electrospun nanofibers were also coated by fluorescent proteins [19] and conducting

polymers [20]. In regard to tissue engineering applications, cell attachment and cell proliferation have been improved by a variety of surface modification techniques [15, 17, and 18], leading to enhanced biocompatibility.

In order to incorporate electrospun nonwoven mats into *in vivo* scaffolds or to use as drug carriers, aliphatic polyesters [21, 22] were probably the most commonly investigated of all available biodegradable and biocompatible polymers. However, in our former study [23] and other researchers' work [24], surface area shrinkage was observed with electrospun PLA fiber mats when the fiber mats were immersed in physiological buffer solution at 37°C. For *in vivo* incorporation, the dimensional stability of the scaffold is critical [25]. Among other attempts, Lee and coworkers [26] used thermal treatments to maintain the area stability and bio-mechanical properties. A further problem is that PDLLA is a hydrophobic material, and electrospun into fibers, could be even more hydrophobic [23], while hydrophilicity is required for tissue engineering scaffolds [27].

Thus, the purpose of this part was to generate nonwoven poly(D, L-lactide) (PDLLA) nanofiber mats that retain a stable area at human physiological conditions, and further to devise a method that would increase their hydrophilicity. We developed a simple physical surface entrapment method to introduce hydrophilic poly(ethylene glycol) (PEG) onto the surface of the nanofibers. The surface area stabilization and PEG introduction were conducted in a one-step process. Both of these two modifications could be critical for electrospun nonwovens as tissue engineering materials in the future. Cell viability tests were performed using canine fibroblasts on the modified fibrous mats.

5.2 Experimental Section

5.2.1 Materials

Poly(D,L-lactide) (PDLLA, Mw=75,000~120,000), poly(ethylene glycol) (PEG, Mw=14,000), 2,2,2-trifluoroethanol (TFE) and benzyltriethylammonium chloride (BTEAC) were obtained from Sigma-Aldrich and used as received. Chloroform (analytical grade) was obtained from Fisher Scientific. 0.05 M Tris buffer solution was prepared from tris(hydroxymethyl)aminomethane hydrochloride (Trizma™ HCl; Sigma-Aldrich) and adjusted to pH 7.35. The MTT cell proliferation assay kit (V-13154) was purchased from Invitrogen and used by following the instructions of the manufacturer.

5.2.2 Electrospinning and surface modification

For electrospinning, 7 wt% PDLLA were dissolved in chloroform by gently stirring at room temperature for at least 12 h. 10 mg of BTEAC was added to the solution to improve the spinnability. For the electrospinning process, a horizontal experimental setup was used, consisting of a syringe, an 18 gauge needle, an aluminum collecting board, and a high voltage supply. A syringe pump connected to the syringe controlled the flow rate to 1 mL/h. PDLLA solution was electrospun at a voltage of 18 kV with a tip-to-collector distance of 15 cm.

For the surface modification, a solution containing 50 wt% PEG, 10 wt% TFE and 40 wt% deionized water was prepared. PDLLA nanofiber mats were immersed in the solution at 42°C for 120 min, followed by washing with a large excess of water to remove the un-trapped PEG. X-ray photoelectron spectroscopy (XPS) was used to estimate surface coverage (see below).

5.2.3 Characterization

The morphology of the electrospun fibers was investigated with a Zeiss DMS 940 scanning electron microscope (SEM) at 15 kV. Electrospun mats were sputter-coated with gold for 2 min to minimize charging effects. The diameters of the fibers were estimated from SEM images.

For surface area shrinkage measurements (*in vitro*) electrospun nonwoven mats were first cut into squares of 20 mm x 20 mm. Then PDLLA nonwoven pieces were immersed in Tris buffer at different set temperatures. At each time interval, dimensions were rapidly measured. After the surface entrapment, the fibrous mats were cut into 10 mm x 10 mm and immersed into Tris buffer at 37 ℃ to test the surface area stability.

A DCA-322 (Cahn Instruments) was used to determine the contact angle of the electrospun fiber mats to water based on the Wilhelmy plate method. Fiber mats were first cut into squares of 10 mm x 10 mm width. To avoid effects caused by fiber swelling, the advancing distance was set to 2 mm with a speed of 80 μm/s and all tests were conducted at room temperature. The tests were done in triplicate and results averaged.

X-ray Photoelectron Spectroscopy (XPS) was utilized to characterize the surface element composition before and after PEG entrapment. The specimens were attached to the AES sample holder by pressing into double-sided sticky tape for high resolution XPS spectra over the C1s feature. The C1s feature was subsequently fitted by XPSPeak 4.1 software with a linear background and Gaussian peak shape.

Canine fibroblasts were cultured in a 75 cm^2 flask L-15 media (Gibco) with antibiotics (Sigma) and 10% fetal bovine serum (Hyclone) essentially as previously described (28, 29). The cells were grown at 100% humidity and 37°C with 5% CO_2. Cells were originally isolated from a biopsy fragment of fascia from the abdominal wall of a normal beagle that was placed in a plate, allowed to attach for approximately 5 min and then 2 ml of media was added to the well. Fibroblasts were allowed to grow out from the biopsy fragment for several days until a monolayer had formed. The media was changed every three days. The cells were harvested by trypsin digestion [28, 29]. The cell number was halved, unused cells frozen for future use and the cell passage numbers recorded. After 20 passages the fibroblasts ceased to grow and a new vial was started.

For each assay, cells were washed with 1xHanks (Sigma) and trypsinized. Initial fibroblast concentration was determined by flow cytometry (Accuri C6) and plated on a piece of sterile gauze in a 24 well plate (50,864 cells/well).

Cell viability on electrospun PDLLA before and after surface modification was determined by 3-(4,5-dimethylthiazol-2-yl)-2,5-diphenyltetrazolium bromide (MTT) (Invitrogen) assay. First, all samples were sterilized by ethanol under a laminar flow hood

before being placed on a 24-well cell culture plate. Then fibroblasts were placed on each well with medium being changed every 2 days. After 1, 3, and 7 days cell seeding, the medium was carefully removed and replaced with 100 μl fresh medium. Then 10 μl of 12 mM MTT solution was added to each well, followed by 4 h incubation at 37°C. 100 μl of SDS-HCl solution was added after the incubation, followed by 10 h incubation. Then the solution in each well was transferred to a 96-well plate and the absorbance read at 570 nm.

5.3 Results and Discussion

The morphology of as-spun PDLLA nanofibers is shown in Figure 4.1(A). Electrospun PDLLA showed a well-formed nonwoven structure with average fiber diameters of 750±320 nm.

Since the glass transition temperature of PDLLA is approximately 55°C [30] and electrospun polymer chains were highly oriented, the nanofibers intended to relax and shrink when the temperature close to the Tg. To study the surface area shrinkage of electrospun fibrous mats, *in vitro* immersion tests in Tris buffer were performed first (Figure 5.1 (B)). As can be seen in Figure 5.1(C), the surface area of PDLLA nonwovens obviously decreased considerably when immersed in buffer solution of a temperature close to the T_g of PDLLA. Hyperbolic-shaped curves were observed when the final area was graphed versus the shrinkage rate. The results significantly depended on the solution temperature. Further, the morphology of nanofibrous mats dramatically changed. Figure 5.1(B) demonstrates that the originally straight fibers had obviously lost stiffness and

elongation due to exposure to buffer at 37°C. It was concluded that in order to create electrospun nonwovens dimensionally stable at human body temperature, the fiber mats needed to be pre-treated at 37°C or higher. Thus, for the subsequent surface entrapment process, a temperature of 42°C was chosen and a treatment time of 120 min to ensure the PDLLA nonwovens did not shrink under physiological conditions.

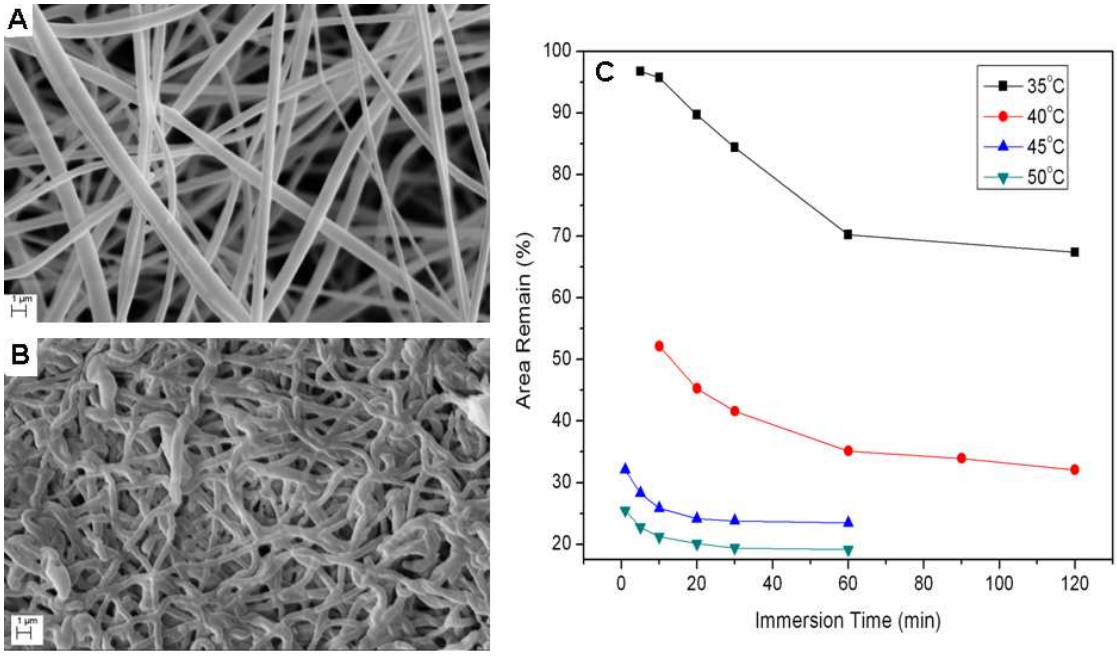

Figure 5.1 (A) SEM image of as-spun PDLLA fibers, (B) SEM image of PDLLA fibrous mat after 2 h immersion in Tris buffer at 37°C, (C) surface area shrinkage of PDLLA mats in Tris buffer at different solution temperatures.

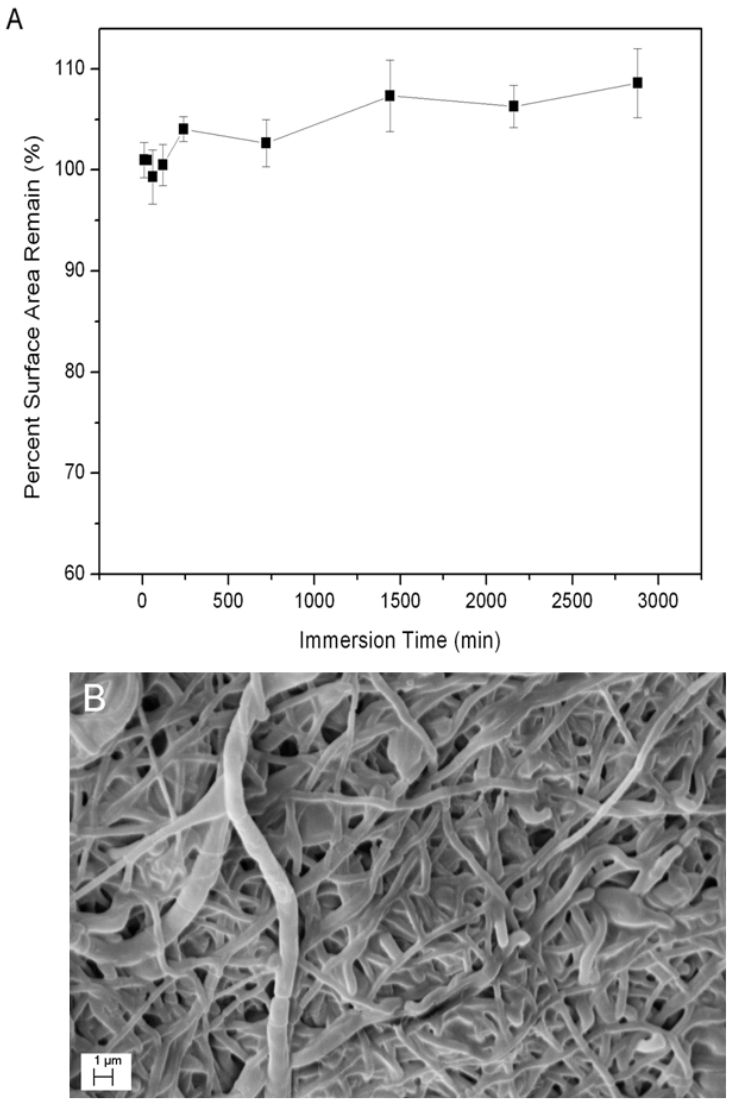

Figure 5.2 (A) Surface area stability of electrospun PDLLA fibrous mats after 2 h PEG entrapment in TFE/water solution at 42°C, (B) SEM image of electrospun PDLLA after PEG entrapment.

Surface entrapment techniques are easy and effective to improve the surface properties, especially for various biocompatible polymers, both in form of films and fibers [31, 32]. Generally, a solvent/nonsolvent system is applied to modify the polymer surfaces through reversible gelation. In this study, TFE/water was selected as the

solvent/nonsolvent mixture for PDLLA. In this system, TFE assists the surface swelling of PDLLA so that PEG is able to diffuse into fiber surface. After the treatment, the fibers are washed with an excess of nonsolvent (water) which causes the swollen structure to collapse. Thus PEG chains were immobilized on PDLLA nanofibers' surfaces.

After surface entrapment at 42°C, the PDLLA nanofiber mats shrunk to approximately 25% of their original size. Then the nonwoven mats were cut into 10 mm x 10 mm specimens and immersed in Tris buffer at 37°C. Their size was measured at each time interval. As can be determined from Figure 5.2(A), the PEG coated ultrafine fiber mats appeared to reach a stable surface area by 12 h. Beyond that, the size of the specimens slightly increased due to the swelling of the PDLLA. Thus, surface entrapment is an effective process to generate surface stable electrospun PDLLA at 37°C.

The morphology of nonwoven fibers after surface entrapment is displayed in Figure 5.2(B). There was no obvious difference of the electrospun fiber mats before (Figure 5.1(B)) and after the surface entrapment process when exposed to Tris buffer. Since the modification was conducted at 42°C, the PEG entrapment occurred along with the surface shrinkage and therefore the fibers remained stable at 37°C.

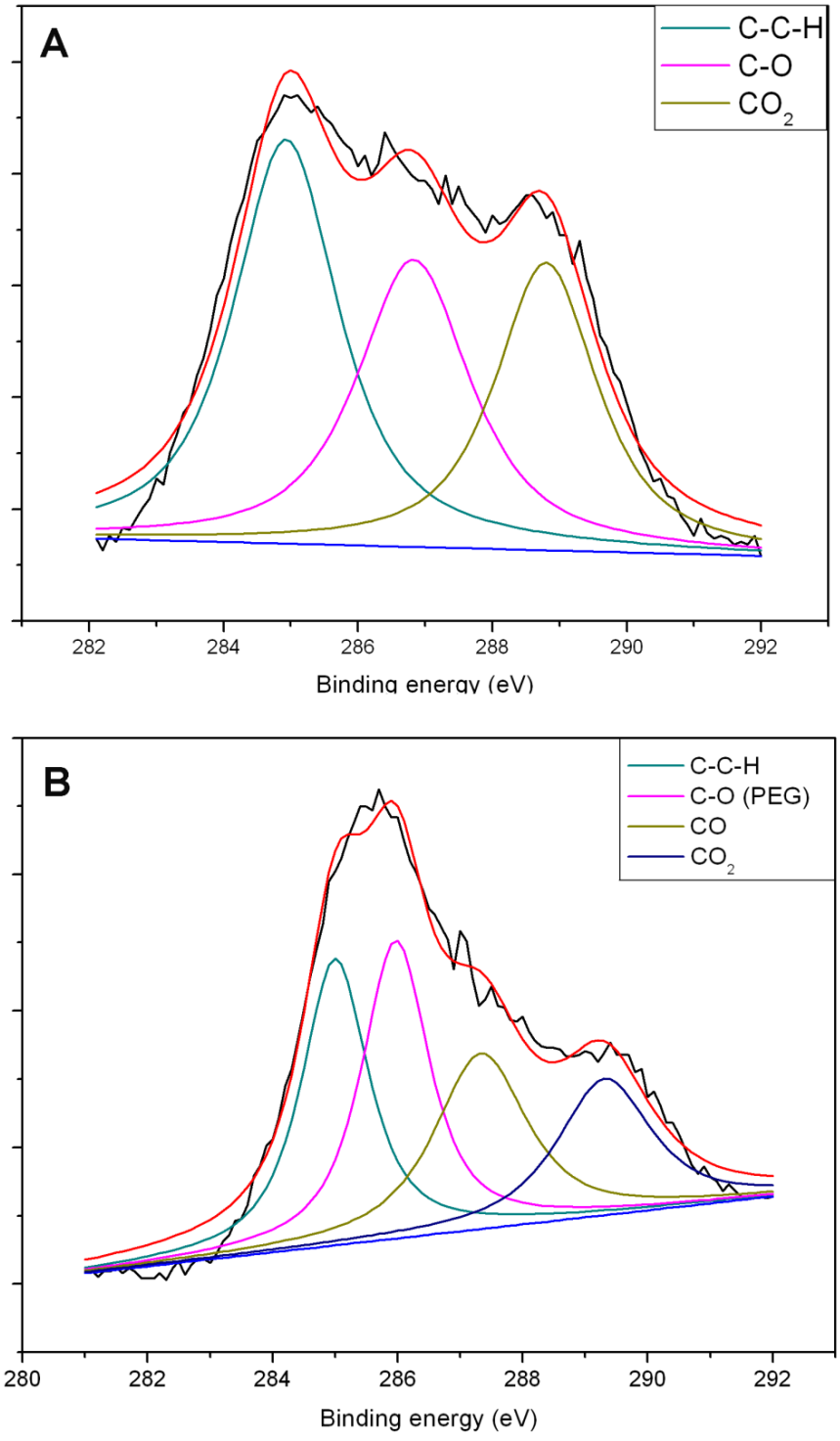

Figure 5.3 XPS C1s scans of PDLLA (A) as-spun, (B) after entrapment of PEG.

High resolution XPS C1s scans were used to determine the surface components of electrospun PDLLA. As shown in Figure 5.3(A), three peaks were identified from the spectrum of as-spun PDLLA fibers. The C-C-H, C-O, and CO_2 groups can be assigned to the peaks of 285, 287, and 289 eV, respectively [31]. After PEG entrapment (Figure 5.3(B)), one more peak appears at about 286 eV, which can be assigned to the C-O ether group of PEG. This result suggests that PEG was successfully coated onto the PDLLA nanofiber surface.

Table 5.1 Curve fitting data from XPS C1s peaks of electrospun PDLLA before and after entrapment modification.

Samples	% peak area				% PEG Surface coverage
	C-C-H	C-O	CO_2	C-O (PEG)	
As-spun PDLLA	40.70	31.20	28.10		
After entrapment	28.13	23.75	18.72	29.40	40.3

Percent peak areas from curve fit of C1s data are shown in Table 5.1. From XPS data, the PEG/PLA monomer ratio can be calculated, which is necessary to estimate the percentage of PEG surface coverage. After 120 min exposure in PEG/water/TFE mixture, 40.3% of the nonwoven mat was covered by PEG.

Accordingly, the water contact angle tests confirmed the effect of the surface modification. The as-spun PDLLA mats showed a contact angle of 125.6±4.0°, while that of PEG coated nonwovens was 34.1±1.9°. The dramatic decrease in contact angle suggests that hydrophilic PEG was indeed coated on the surface of the nanofibers. The resultant hydrophilicity is crucial for future applications as biomedical materials.

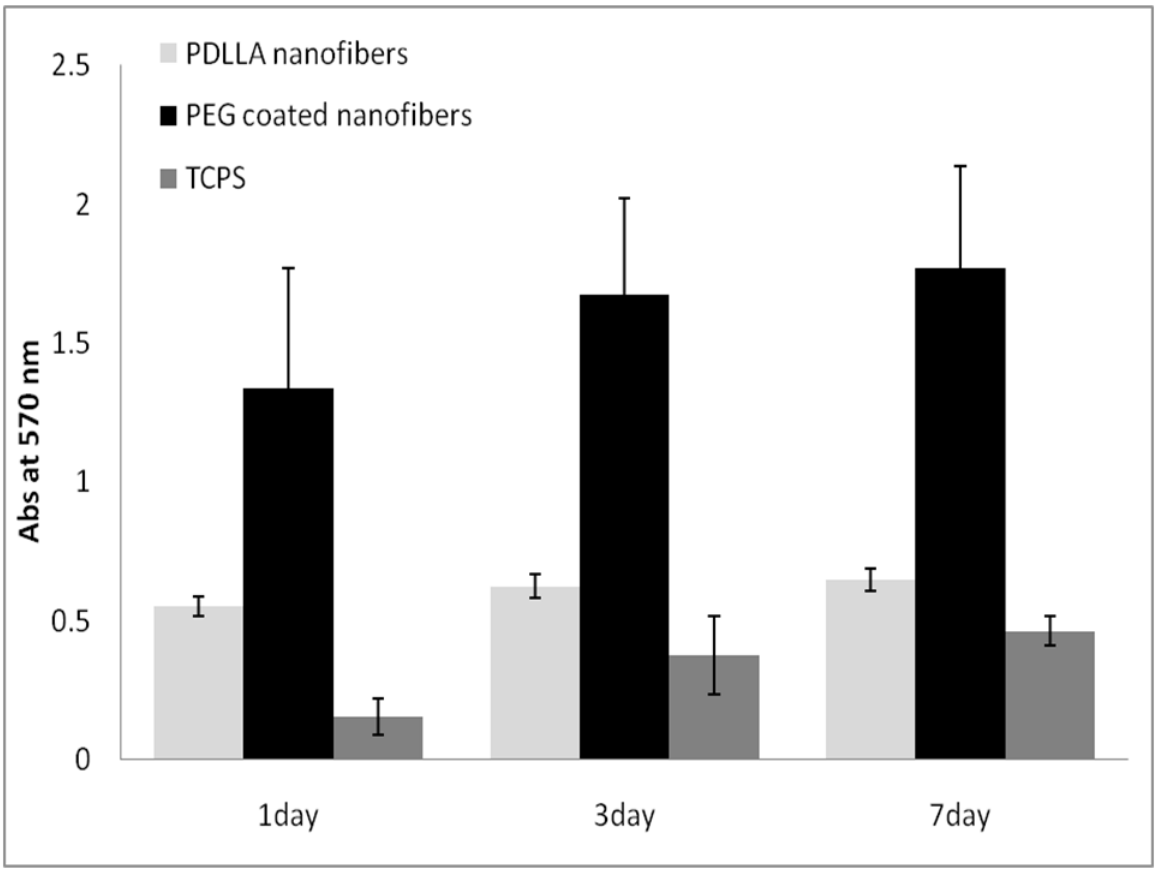

Figure 5.4 MTT viability on as-spun PDLLA nanofibers, PEG coated nanofibers and TCPS (24-well tissue culture plates).

Canine fibroblasts were used via MTT assay to investigate whether cell viability had improved after surface modification. The results are summarized in Figure 5.4, with tissue culture plates (TCPS) as control. Fig. 4 shows that with longer incubation period,

cell growth gradually increased on all substrates which was to be expected. However, lower absorbance was observer on TCPS controls due to the formation of a monolayer of cells. Fibroblasts clearly proliferated better on electrospun PDLLA nanofibers due to their porous structure. The absorbance was approximately four times higher on the nanofibers than on the controls. It needs to be pointed out, however, that the improvement was limited by the shrinkage of fiber mats. As shown in Figure 5.4, after the modification of PEG entrapment, the cell proliferation dramatically increased by 2-3 fold. Thus, it is clear that both the surface stabilization and the enhanced hydrophilicity enhanced cell adhesion and growth on the modified PDLLA nanofibrous scaffold.

5.4 Conclusions

In this study, PDLLA ultrafine fibers were created by electrospinning. Surface area shrinkage and temperature dependence of as-spun fiber mats were evaluated. PEG was successfully coated onto PDLLA nanofibers by physical surface entrapment, and characterized by XPS and water contact angle tests. As indicated by XPS analysis, after 120 min treatment, 40.3% of surface was covered by PEG. As expected, electrospun fiber mats changed from hydrophobic to hydrophilic. Simultaneously, since surface entrapment was conducted in 42°C, the final product also showed a stable area at 37°C, which is the human body temperature. MTT assay confirmed that the cell viability increased by PEG entrapment due to the improvement of dimensional stability and enhanced hydrophilicity. Thus, after surface entrapment, PEG coated polymeric nanofibers could serve as potential scaffold materials for tissue engineering applications.

5.5 References

1. Greiner A.; Wendorff J. H. Angew. Chem. Int. Edn. 2007, 46, 5670.
2. Sill T. J.; von Recum H. A. Biomaterials 2008, 29, 1989.
3. Doshi J.; Reneker, D. H. J Electrostatics 1995, 35, 151.
4. Shin, Y. M.; Hohman, M. M.; Brenner, M. P.; Rutledge, G. C. Polymer 2001, 42, 9955.
5. Gopal R.; Kaur S.; Feng C. Y.; Chan C.; Ramakrishna S.; Tabe S.; Matsuura T. J. Membr. Sci. 2007, 289, 210.
6. Patel A. C.; Li S.; Wang C.; Zhang W.; Wei Y. Chem. Mater. 2007, 19, 1231.
7. Onozuka K.; Ding B.; Tsuge Y.; Naka T.; Yamazaki M.; Sugi S.; Ohno S.; Yoshikawa M.; Shiratori S. Nanotechnology 2006, 17, 1026.
8. Kidoaki, S.; Kwon, I. K.; Matsuda, T. Biomaterials 2005, 26, 37.
9. Sell, S.; Barnes, C.; Smith, M.; McClure, M.; Madurantakam, P.; Grant, J.; McManus, M.; Bowlin, G. L. Polym. Int. 2007, 56, 1349.
10. Chen, J. P.; Chang, G. Y.; Chen, J. K. Coll. and Surf. A: Phys. Eng. Asp. 2008, 313-314, 183.
11. Goldburg M.; Lager R.; Jia X. Q. J. Biomater. Sci. Polym. Edn. 2007, 18, 241.
12. Carpenter J.; Khang D.; Webster T. J. Nanotechnology 2008, 19, 505103.
13. Kim G.; Park J.; Park S. J. Polym. Sci. B: Polym. Phys. 2007, 45, 2038.
14. Sun X. Y.; Shankar R.; Böner H. G.; Ghosh T. K.; Spantak R. J. Adv. Mater. 2007, 19, 87.
15. Chen F.; Lee C. N.; Teoh S. H. Mater. Sci. Eng. C 2007, 27, 325.
16. Ma Z. W.; Kotaki M.; Ramakrishna S. J. Membr. Sci. 2006, 272, 179.

17. Prabhakaran M. P.; Venugopal J.; Chan C. K.; Ramakrishna S. Nanotechnology 2008, 19, 455102.

18. Ma Z. W.; Kotaki M.; Yong T.; He W.; Ramakrishna S. Biomaterials 2005, 26, 2527.

19. Choi J. S.; Yoo H. S. J. Bioact. and Comp. Polym. 2007, 22, 508.

20. Nair S.; Hsiao E.; Kim S. H. J. Mater. Chem. 2008, 18, 5155.

21. Zhu X.; Cui W.; Li X.; Jin Y. Biomacromolecules 2008, 9, 1795.

22. Luong-Van E.; Grondahl L.; Chua K. N.; Leong K. W.; Nurcombe V.; Cool S. M. Biomaterials 2006, 27, 2042.

23. Xie Z. W.; Buschle-Diller G. J. Appl. Polym. Sci. 2010, 115, 1.

24. Jiang, H. L.; Wang, D. F., Hsiao, B; Chu, B; Chen, W. L. J. Biomater. Sci. Polym. Edn. 2004, 15, 279.

25. Zhu Y. B.; Gao C. Y.; Liu X. Y.; Shen J. C. Biomacromolecules 2002, 3, 1312.

26. Lee S. J.; Oh S. H.; Liu J.; Soker S.; Atala A.; Yoo J. J. Biomaterials, 29, 2008, 1422.

27. Atthoff B.; Hilborn J. J. Biomed. Mater. Res. B: Appl. Biomater. 2007, 80B, 121.

28. Bird, R. C.; Church-Bird, A.; DeInnocentes, P. In Nature: Encyclopedia of the Life Sciences, John Wiley & Sons: New Jersey, 2005, 1.

29. DeInnocentes, P.; Li, L. X.; Sanchez, R. L.; Bird, R. C. Vet. Comp. Oncol. 2006, 4, 161.

30. Chasin M.; Langer R. Biodegradable Polymers as Drug Delivery Systems; Marcel Dekker Inc.: New York, NY 1990

31. Quirk R. A.; Davies M. C.; Tendler S. J.; Chan W. C.; Shakesheff K. M.

Langmuir 2001, 17, 2817.

32. Hou, Q.; Freeman R.; Buttery L. D.; Shakesheff K. M. Biomacromolecules 2005, 6, 734.

CHAPTER 6 CHEMICAL SURFACE MODIFICATION OF ELECTROSPUN NANOFIBERS

6.1 Introduction

With the development of biomaterials, surface property became a critical issue with significant influence on biocompatibility and bioactivity [1]. Both surface chemistry [2] and surface morphology [3] are important to determine the performance of the biomaterials, especially in the case of polymers. In most researches, polymeric scaffolds were modified by proteins [4], polyelectrolytes [5], and growth factors [6]. One of the most effective tools to fine-tune surface chemistry is surface etching. Zhu et al, [7] and Croll et al, [8] discovered that by surface etching and further binding with proteins, cell attachment and proliferation significantly improved on biodegradable polyesters. Ohe and coworkers [9] also proved that similar technique can be used to modify commercial fiber surfaces.

In recent years, electrospinning has been studied as an extremely promising method to prepare tissue engineering scaffolds [10, 11]. Electrospun nanofibers can provide high surface area and 3D porous structure as a mimic of extracellular matrix (ECM). Although biodegradable polymers can be easily electrospun into nanofibrous mats, there are still

some critical issues remaining, for example, surface properties. Efforts were made to functionalize the surface of electrospun nanofibers.

Different approaches were applied to modify the surfaces of polymeric nanofibers during or after electrospinning. The first effort by Casper et al, [12] was based on electrospinning of a mixed polymer solution to get the desired polymer located on the surface of fibers. A double-nozzle setup was used to get poly(ethylene oxide) (PEO) coated poly(ε-caprolactone) (PCL) nanofibers [13]. Ma et al, [14] conducted air plasma treatment to attach bovine serum albumin (BSA) on the surface of electrospun polysulphone surface to improve its affinity. The same research group treated PCL nanofibrous mats with a similar method to get a better performance for nerve tissue engineering [15]. Another major method of surface modification is surface etching. Ma and coworkers [16] etched polyethylene terephthalate nanofibers by formaldehyde and further bonded gelatin. They found that the cell attachment and proliferation improved considerably, as required by blood vessel engineering. Choi and Yoo [17] prepared BSA-immobilized PCL nanofibers via amine etching treatment also.

On the other hand, electrospun nanofibers of conducting polymers gained the interest of researchers in recent years [18, 19]. It was proved that conducting polymers, for example polypyrrole (Ppy) and polyaniline (PANI) are compatible and suitable for biomedical applications, especially for guided nerve tissue regeneration [20, 21]. However, pure conducting polymers are not easy to be dissolved and electrospun. Thus, coating electrospun biodegradable nanofibers with conducting polymers is a rational routine to generate good fiber morphology and mechanical strength. Dong and Jones [22] prepared Ppy/poly(methyl methacrylate) (PMMA) coaxial fibers by depositing Ppy on

PMMA nanofibers in water. Xie et al, [23] fabricated Ppy coated PCL and PLLA nanofibers through a similar process. They also observed oriented neuritis growth along fibers, suggesting potential guided nerve tissue regeneration. Nair et al, [24] demonstrated that polystyrene/Ppy core-shell nanofibers can be made by electrospinning and further coating in vapor phase. Moreover, Abidian and cowokers [25] coated drug loaded PLLA nanofibers with poly(3,4-ethylenedioxythiophene) (PEDOT), which is another conducting polymer. As a result, the drug release profile was controlled by electrical signal via microelectrodes.

In this chapter, two approaches were applied to functionalize the surface of electrospun fibers. Firstly, electrospun PCL nanofibers were treated by 1, 6-hexanediamine, and then glutaraldehyde, which provided the aldehyde groups that further reacted with chitosans and proteins. The surface composition was analyzed by X-ray photoelectron spectroscopy. Secondly, electrospun PDLLA was coated by Ppy via in-situ polymerization in aqueous solution. Also, in order to prepare Ppy nanotubes, PDLLA nanofibers were removed by immersion in dichloromethane (DCM). The morphology of the core-shell fibers and nanotubes were observed by scanning electron microscopy (SEM) and transmission electron microscopy (TEM). Surface chemistry was identified by Fourier Transform Infrared Spectroscopy (FTIR).

6.2 Experimental Section

6.2.1 Materials

Poly(ε-caprolactone) (PCL, Mw=80,000) and poly(D,L-lactide) (PDLLA, Mw=75,000~120,000), Chitosan (Medium Mw grade), and collagen (soluble, Type I) was purchased from Sigma-Aldrich. Chloroform, 2-propanol, glutaraldehyde (GA), dichloromethane and ferrous chloride were obtained from Fisher Scientific. 1.6-hexanediamine, benzyltriethylammonium chloride (BTEAC), 1,3-dioxane and ninhydrin solution were also bought from Sigma-Aldrich. The pyrrole monomers were provided by Dr. Xinyu Zhang.

6.2.2 Electrospinning

The electrospinning process was similar to previous projects. 5 wt% PDLLA or 5 wt% PCL were dissolved in chloroform by gently stirring at room temperature for at least 12 h. 10 mg of BTEAC was added to the solution to improve the spinnability. For the electrospinning process, a horizontal experimental setup was used, consisting of a syringe, an 18 gauge needle, an aluminum collecting board, and a high voltage supply. A syringe pump connected to the syringe controlled the flow rate to 1 mL/h for PDLLA and 0.5 mL/h for PCL. PDLLA solution was electrospun at a voltage of 18 kV with a tip-to-collector distance of 15 cm.

6.2.3 Chemical surface modification

For surface etching modification, a piece of dry electrospun PCL fiber mat was immersed in 10 wt% 1, 6-hexanediamine/2-propanol solution for certain time at 40 °C, then rinsed with a large amount of deionized (DI) water for several hours. After drying in air, the nanofibrous mat was immersed in 1 wt% GA solution for 3 h at room temperature,

followed by washing with DI water for several hours. Then the membrane was incubated in 2 mg/mL chitosan solution or 2 mg/mL collagen solution for 24 h at 2-4 °C. After the reaction, the PCL membrane was rinsed by 1% acetic acid first, and then by a large amount of DI water for several hours.

For Ppy coating, a piece of electrospun PDLLA mat was immersed in a 10 mL 0.05 M pyrrole aqueous solution. The polymerization was initiated by adding 10 mL $FeCl_3$ solution (84 mM), in which Fe^{3+} was an oxidant and Cl^- was a dopant. The reaction was conducted under vigorous stirring for 1 h, while the fiber mat turned black. After that, PDLLA fibers were rinsed by DI water for several hours to remove the loosely attached Ppy particles. In order to prepare Ppy nanotubes, a piece of Ppy-PDLLA core-shell fiber mat was immersed in dichloromethane for 24 h in room temperature under gentle shaking.

6.2.4 Characterization

The amount of amine groups on the surface of PCL after etching was determined by the ninhydrin analysis. One piece of etched PCL nanofibrous mat with the size of 10 x 10 mm was immerse in 1M ninhydrin solution for 1min, then heated to 80 °C for 15 min to accelerate the reaction. 5 mL 1, 4-dioxane was added to dissolve the polymer, followed by another 5 mL of 2-propanol to stabilize the reaction. The absorbance was tested by a UV-vis spectroscopy at 538 nm. A calibration curve was prepared with pure 1,6 hexanediamine in a 1,4-dioxane/2-propanol solution.

The morphology of the electrospun fibers was investigated with a Zeiss DMS 940 scanning electron microscope (SEM) at 15 kV. Electrospun PDLLA and PCL mats were

sputter-coated with gold for 2 min to minimize charging effects. The sputter-coating was not necessary for Ppy coated nanofibers. The diameters of the fibers were estimated from SEM images. The Ppy nanotubes was observed by a Zeiss EM 10 CR transmission electron microscopy (TEM) at 80 kV accelerating voltage. The sample was prepared by dispersing a little piece of Ppy nanotube mat in water/ethanol solution, and then a small drop of the dispersion was placed on a copper mesh and dried in air.

X-ray Photoelectron Spectroscopy (XPS) was utilized to characterize the surface element composition before and after the surface modification. The specimens were attached to the AES sample holder by pressing into double-sided sticky tape for the scanning of all elements. The result was subsequently fitted by XPSPeak 4.1 software with a linear background and Gaussian peak shape. A Thermo Scientific Nicolet 6700 Fourier Transform Infrared Spectroscopy (FTIR) with an Attenuated Total Reflection (ATR) component was used to test the surface functional groups.

6.3 Results and Discussion

Scheme 6.1 Molecule structure of Poly(ε-caprolactone) (PCL)

The molecule structure of PCL is shown in Scheme 6.1. Since PCL is a crystalline polymer and that the aminolysis temperature in this case was 40°C (lower than the aminolysis temperature in chapter 4), only the surface of PCL was etched instead of

broken into particles. The morphology of electrospun PCL was similar to above-mentioned PLLA nanofibers with a diameter of about 500 nm. The nonwoven fibrous structure makes these nanofiber mats an excellent candidate for tissue engineering. However, surface chemistry and affinity still need to be improved. Figure 6.1 illustrated the first strategy used for chemical surface modification. First, -NH_2 groups were introduced on electrospun PCL membranes by aminolysis. The existence of amine groups was proved by XPS, as shown in Table 6.1. Second, these amine groups were reacted with glutaraldehyde, which was further reacted with the amine groups of biomacromolecules, like chitosan or collagen. The success of surface immobilization was proved by XPS (Table 6.1), as more nitrogen was observed on surface.

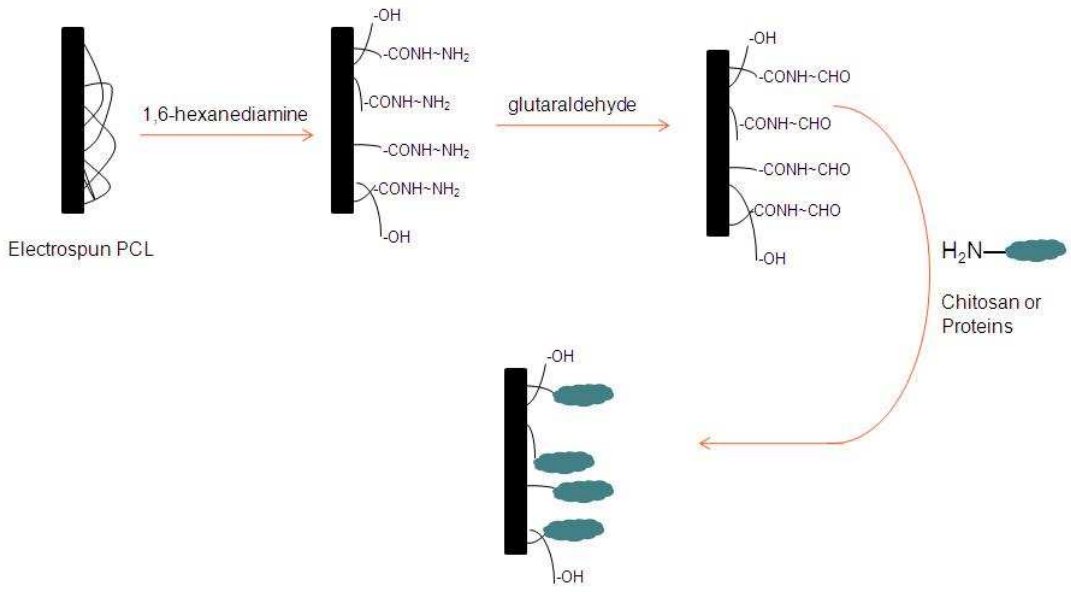

Figure 6.1 Illustration of surface etching and modification of electrospun PCL nanofibers.

Tabe 6.1 Surface elemental composition determined by XPS

Surface Elemental Composition (atom %)			
Element	O	N	C
ES PCL Control	14.57	0.0	78.00
ES PCL-NH_2	14.00	0.51	79.03
ES PCL-Chitosan	15.81	3.11	81.08
ES PCL-Collagen	14.98	3.88	73.56

The quantitative amount of -NH_2 groups on aminolyzed PCL membranes was investigated by ninhydrin analysis. Ninhydrin reacted with NH_2 resulted in a blue product. As shown in Figure 6.2, the density of -NH_2 groups on electrospun PCL surface was increased with longer aminolysis time until saturated at 4 h. Thus, all surface modifications were conducted with 4 h aminolysis.

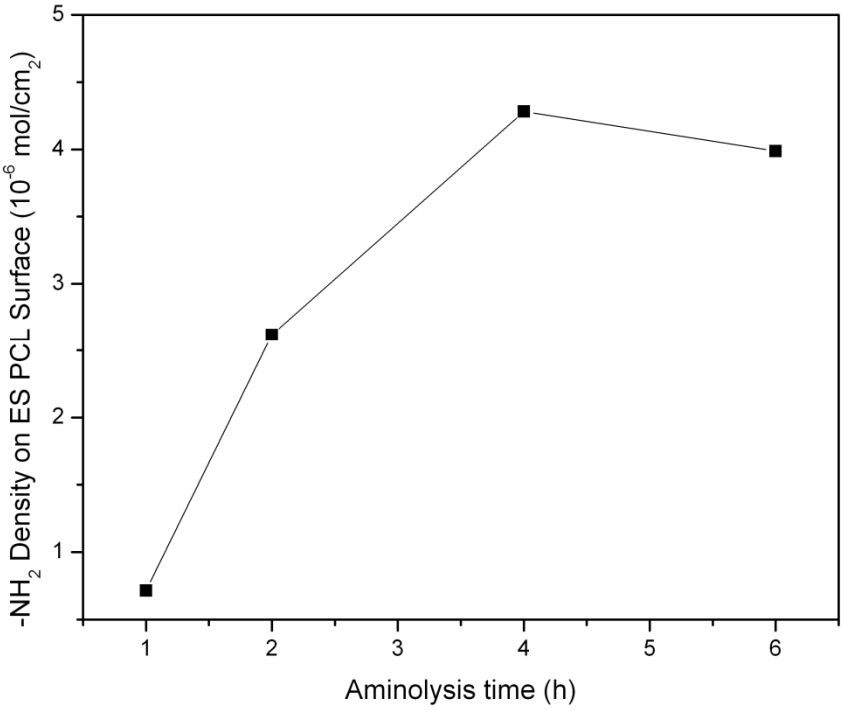

Figure 6.2 The density of amine groups on surface of electrospun (ES) PCL after different etch times.

As mentioned above, after surface etching and further reaction, chitosan and collagen were immobilized on electrospun PCL nanofibers, as supported by XPS data (Table 6.1). It could be demonstrated by several researchers [4, 7, 8] that surface attachment of biological macromolecules can help improve cell attachment and proliferation, which are critical for tissue engineering. Thus, the surface modified PCL nanofibers could be more valuable tissue engineering in the future.

Another aspect of this project was to coat electrospun PDLLA nanofibers with conducting polymer. The morphology of PDLLA fibers before and after Ppy coating is displayed in Figure 6.3. Electrospun PDLLA nanofibers exhibited a smooth and uniform

morphology with a diameter of 277.5 nm on the average. After coating with Ppy, the nonwoven fibrous structure remained. However, some Ppy granules can be observed on the core-shell fibers, which have an average diameter of 356.99 nm. Thus, the thickness of the outer layer of Ppy is 39.75 nm.

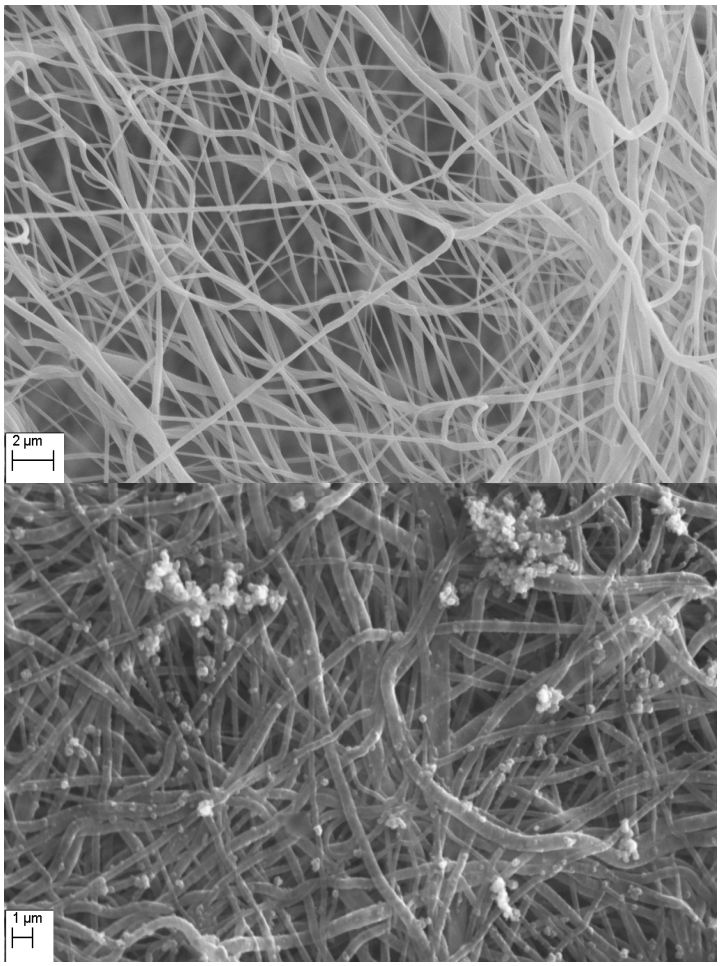

Figure 6.3 SEM images of electrospun PDLLA nanofibers before (A) and after Ppy coating (B).

The chemical composition was identified by FTIR. As shown in Figure 6.4, electrospun PDLLA showed the typical IR spectrum with characteristic peaks at 3377 cm^{-1} (O-H stretching) and 1753 cm^{-1} (C=O stretching). With Ppy coating, some strong

peaks of PLA still remained, for example, the C=O stretching peak. Additionally, new peaks at 1537 and 1450 cm^{-1} could be observed, corresponding to the C=C stretching of pyrrole. Therefore, with the observation by FTIR, the chemical coating of conducting polymers was confirmed.

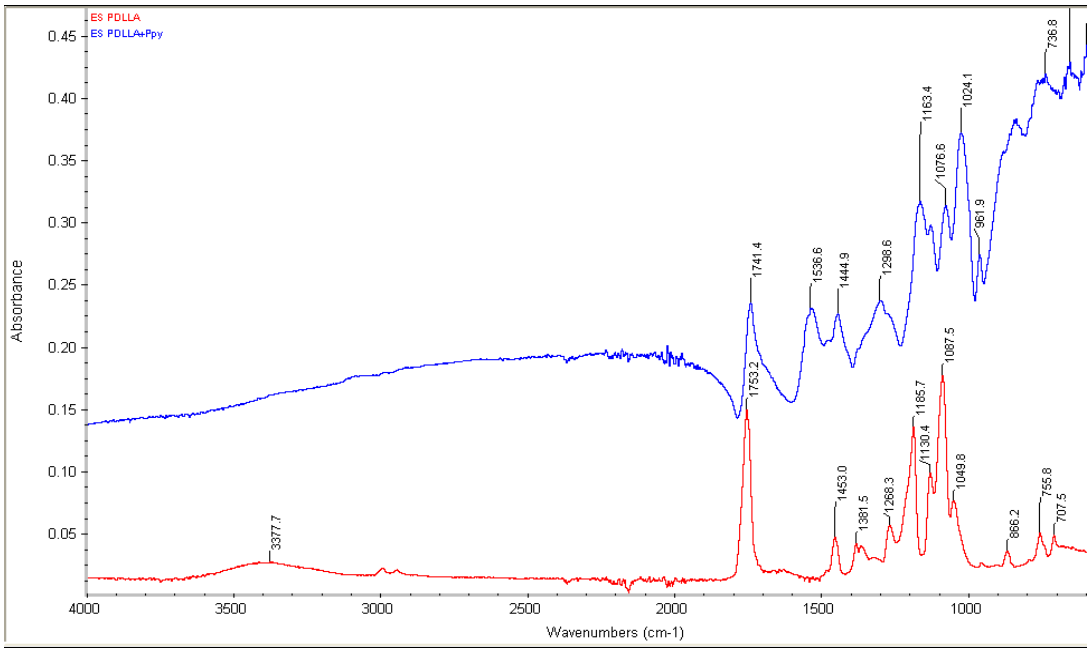

Figure 6.4 FTIR spectrum of electrospun PDLLA before and after Ppy coating.

After the removal of the PDLLA nanofibrous templates, Ppy nanotubes were fabricated. The structure was revealed by TEM (Figure 6.5). It was clear that a hollow tubular structure was formed in large amounts. Here, a nonwoven mesh is almost formed. By closer observation, some Ppy granules also exist on the surface of the nanotubes. The average outer diameter was 229.20 nm, while the inner diameter was 139.62 nm. Thus, the wall thickness of Ppy nanotubes resulted in 44.79 nm, which is almost the same result determined by SEM. These Ppy nanotubes can be further modified into carbon nanotubes by pyrolysis under inert gas atmosphere [26].

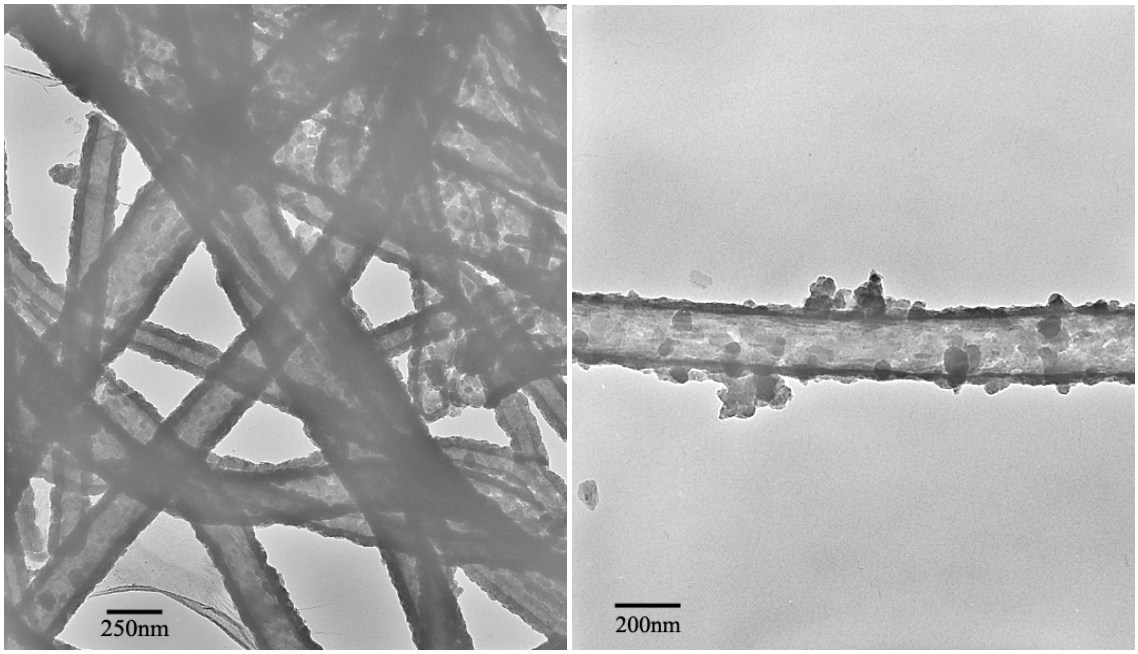

Figure 6.5 TEM images of Ppy nanotubes.

6.4 Conclusion

In conclusion, two routines were applied to modify and functionalize the surface of electrospun polymeric nanofibers. First, electrospun PCL nanofibers were attached to biomacromolecules by chemical binding via a three-step reaction. As the first and most important step, amine groups were generated on PCL surface by aminolysis. A level of saturation was achieved after aminolysis of 4 hours. The XPS confirmed that chitosan and collagen were successfully attached on electrospun nanofibers after the modification. The functionalized PCL nanofibers could play a significant role in tissue engineering. Second, polypyrrole was successfully coated on electrospun PDLLA nanofibers by in-situ polymerization with a coating thickness of approximately 40 nm. By removal of the electrospun template, Ppy nanotubes were fabricated with a wall thickness of 40-45 nm.

These core-shell fibers and nanotubes might have a large variety of potential applications in drug delivery, nerve tissue engineering, actuators and supercapacitors.

6.5 References

1. Ratner B.D.; Hoffman A.S.; Schoen F.J.; Lemons J.E. Biomaterials science: An introduction to materials in medicine; Elsevier: London, 2004.
2. Atthoff B.; Hilborn J. J. of Biomed. Mater. Res. B: Appl. Biomater. 2007, 80B, 121.
3. Carpenter J.; Khang D.; Webster T.J. Nanotechnology 2008, 19, 505103.
4. Zhu Y.; Chian K.S.; Chan-Park M.B.; Mhaisalkar P.S.; Ratner B.D. Biomaterials 2006, 27, 68.
5. Lin Y.; Wang L.; Zhang P.; Wang X.; Chen X.; Jing X.; Su Z. Acta Biomater. 2006, 2, 155.
6. Chung T-W.; Yang M-G.; Liu D-Z.; Chen W-P.; Pan C-I.; Wang S-S. J. of Biomed. Mater. Res. A 2005, 72A, 213.
7. Zhu Y.; Gao C.; Liu X.; Shen J. Biomacromolecules 2002, 3, 1312.
8. Croll T.I.; O'Connor A.J.; Stevens G.W.; Cooper-White J.J. Biomacromolecules 2004, 5, 463.
9. Ohe T.; Yoshimura Y.; Abe I. Tex. Res. J. 2007, 77, 131.
10. Sell S.; Barnes C.; Smith M.; McClure M.; Madurantakam P.; Grant J.; McManus M.; Bowlin G. Polym. Int. 2007, 56, 1349.
11. Agarwal S.; Wendoff J.H.; Greiner A. Adv. Mater. 2009, 21, 3343.
12. Casper C.L.; Yamaguchi N.; Kiick K.L.; Rabolt J.F. Biomacromolecules 2005, 6, 1998.

13. Kim G.; Park J.; Park S. J. of Polym. Sci. B: Polym. Phys. 2007, 45, 2038.

14. Ma Z.; Kotaki M.; Ramakrishma S. J. of Membr. Sci. 2006, 272, 179.

15. Prabhakaran M.P.; Venugopal J.; Chan C.K.; Ramakrishma S. Nanotechnology 2008, 19, 455102.

16. Ma Z.; Kotaki M.; Yong T.; He W.; Ramakrishma S. Biomaterials 2005, 26, 2527.

17. Choi J.S.; Yoo H.S. J. of Bioact. & Compat. Polym. 2007, 22, 508.

18. Attout A.; Yunus S.; Bertrand P. Polym Eng. & Sci. 2008, 48, 1661.

19. Cardenas J.R.; de Franca M.G.O.; de Vasconcelos E.A.; de Azevedo W.M.; da Silva E.F. J. Phys. D: Appl. Phys. 2007, 40, 1068.

20. Guimard N.K.; Gomez N.; Schmidt C.E. Prog. In Polym. Sci. 2007, 32, 876.

21. Kotwal A.; Schmidt C.E. Biomaterials 2001, 22, 1055.

22. Dong H.; Jones W.E. Langmuir 2006, 22, 11384.

23. Xie J.; MacEwan M.R.; Willerth S.M.; Li X.; Moran D.W.; Sakiyama-Elbert S.E.; Xia Y. Adv. Funct. Mater. 2009, 19, 2312.

24. Nair S.; Hsiao E.; Kim S.H. J. of Mater. Chem. 2008, 18, 5155.

25. Abidian M.R.; Kim D-H.; Martin D.C. Adv. Mater. 2006, 18, 405.

26. Shang S.; Yang X.; Tao X-M. Polymer 2009, 50, 2815.